JOURNAL OF GEOPHYSICAL RESEARCH, VOL. 104, NO. C12, PAGES 29,925–29,949, DECEMBER 15, 1999

Influences of physical processes on the ecosystem in Jiaozhou Bay: A coupled physical and biological model experiment

Changsheng Chen, Rubao Ji, Lianyuan Zheng
Department of Marine Sciences, University of Georgia, Athens

Mingyuan Zhu
First Institute of Oceanography, State Oceanic Administration, Qingdao, P. R. China

Mac Rawson
School of Marine Programs, University of Georgia, Athens

Abstract. In this paper we have used a three-dimensional coupled physical and biological model to examine the marine ecosystem of Jiaozhou Bay. Physical processes included (1) the M_2 tide, (2) river discharges, and (3) winds. The biological model described a simple, phosphorous-based, lower trophic food web system. The model results showed that tidal mixing had a direct impact on temporal and spatial distributions of nutrients and phytoplankton as well as on shellfish aquaculture. Nutrients and phytoplankton were well mixed vertically by tidal motion. Their concentrations were highest around northwestern and northern regions of the bay near river sources and decreased with water depth from the inner bay to the outer bay. A phytoplankton bloom can occur around the northwestern coast due to the "accumulation" of nutrients under southeasterly wind conditions. The flux analysis suggests that in summer the nutrients in Jiaozhou Bay was directly supplied and maintained by physical processes, but the temporal variation of phytoplankton was controlled dominantly by biological processes associated with nutrient uptake, grazing by zooplankton, and consumption by shellfish. Shellfish aquaculture can modify the bay-scale balance of the ecosystem in Jiaozhou Bay. The loss of phytoplankton in shellfish aquaculture sites tended to be compensated by advection and diffusion from the surrounding waters. A large consumption of phytoplankton by shellfish can cause a net flux of phytoplankton from the Yellow Sea to Jiaozhou Bay, although there was a net nutrient flux flowing out of the bay. The physical mechanism for the water exchange between Jiaozhou Bay and the Yellow Sea was controlled mainly by a chaotic process associated with nonlinear interactions between oscillating tidal currents and double residual eddies.

1. Introduction

Jiaozhou Bay, located on the western coast of the Yellow Sea (YS), People's Republic of China (35°38'-36°18'N, 120°04'-120°23' E), is a shallow semiclosed bay with a total area of ~400 km^2 and an average water depth of 7 m (Figure 1). The maximum water depth is over 50 m at the center of the strait, a passage to the YS. This bay also is characterized by a large intertidal zone (which is dry during the ebb tide and wet during the flood tide) in the northwestern and northern areas where several large rivers terminate. Recently, the coastline on the eastern side of Jiaozhou Bay has shifted slightly offshore due to land reclamation for a highway construction around the bay.

The physical processes that mainly control the temporal and spatial variations of the ecosystem in Jiaozhou Bay include (1) tides, (2) wind, and (3) river discharges. The semidiurnal M_2 tide is a dominate tidal component which accounts for ~80-90% of current variation and kinetic energy inside the bay [*Ding*, 1992]. The average tidal current is over 15 cm s^{-1}, with a maximum of 150 cm s^{-1} occurring at the entrance of the bay. The tide creates strong turbulent mixing, which significantly contributes to the vertically homogenized profiles of temperature, salinity, and biological variables over the year [*Weng et al.*, 1992].

The wind varies significantly with seasons. The entire bay is dominated by a southerly or southeasterly wind in spring and summer and by a northerly or northwesterly wind in fall and winter. The climatologically averaged wind speed is ~5 m s^{-1} in summer and ~7 m s^{-1} in winter [*Zhao et al.*, 1995]. Wind-induced currents play a significant role in the bay-scale water transport near the surface, especially in the shallow region where the tidal residual current is weak.

Six major rivers terminate around the coast of Jiaozhou Bay. Freshwater discharges from these rivers vary seasonally, with a maximum of 135 m^3 s^{-1} occurring in August [*Marine Environmental Monitoring Center*, 1992]. The largest river is the Dagu River located on the western side of the bay. The output of this river recorded in August 1991 was 113 m^3 s^{-1}, which accounted for 84% of the total river discharges in the bay during that summer.

Paper number 1999JC900203
0148-0227/99/1999JC900203$09.00

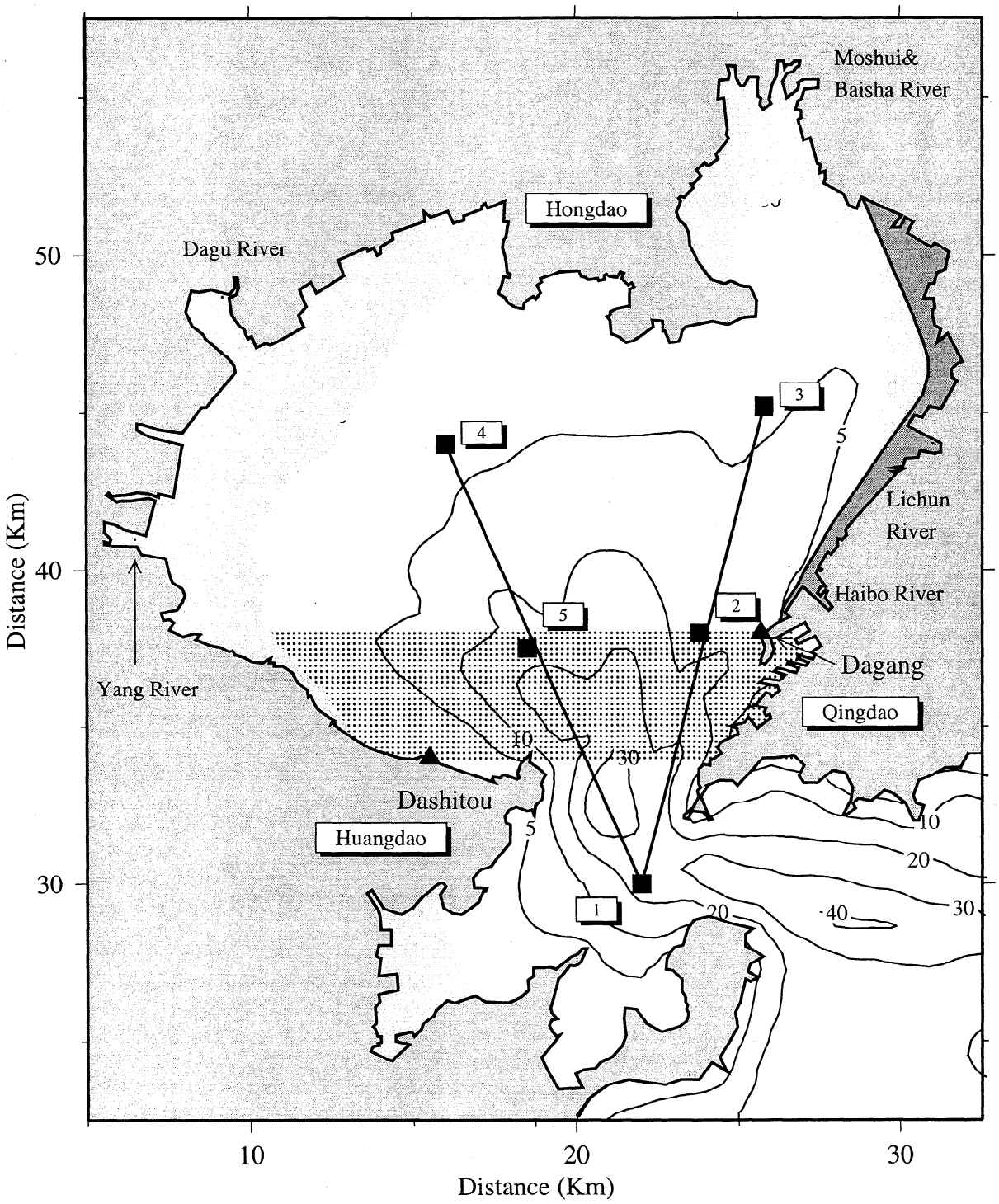

Figure 1. Bathymetry (in meters) of Jiaozhou Bay, Qingdao, China. The solid squares are the biological measurement stations. The heavy solid lines are the sections for the model-data comparison. The solid triangles are tidal measurement stations. The light gray area indicates the intertidal zone. Locations of six major rivers are indicated by solid circles. Dotted area indicated the initial locations of particles released at the 10th model day.

The biological field in Jiaozhou Bay has changed dramatically in the last three decades due to the proliferation of industries, aquaculture, agriculture, and domestic sewage around or inside the bay [*Liu*, 1992]. For example, annually averaged concentrations of total inorganic nitrogen and phosphate have increased from 1.2 and 0. 14 μmol L^{-1} in 1962-1963 to 10.4 and 0.45 μmol L^{-1} in 1992. The atomic ratio of total inorganic nitrogen to phosphate was ~10 in 1962-1963, but is now up to 24.2. Nitrogen used to be a requisite component for the growth of phytoplankton in Jiaozhou Bay, but now the bay has turned into a phosphorous-limited ecosystem [*Shen*, 1995].

The temporal and spatial variations of phytoplankton in Jiaozhou Bay are closely related to the light intensity, the

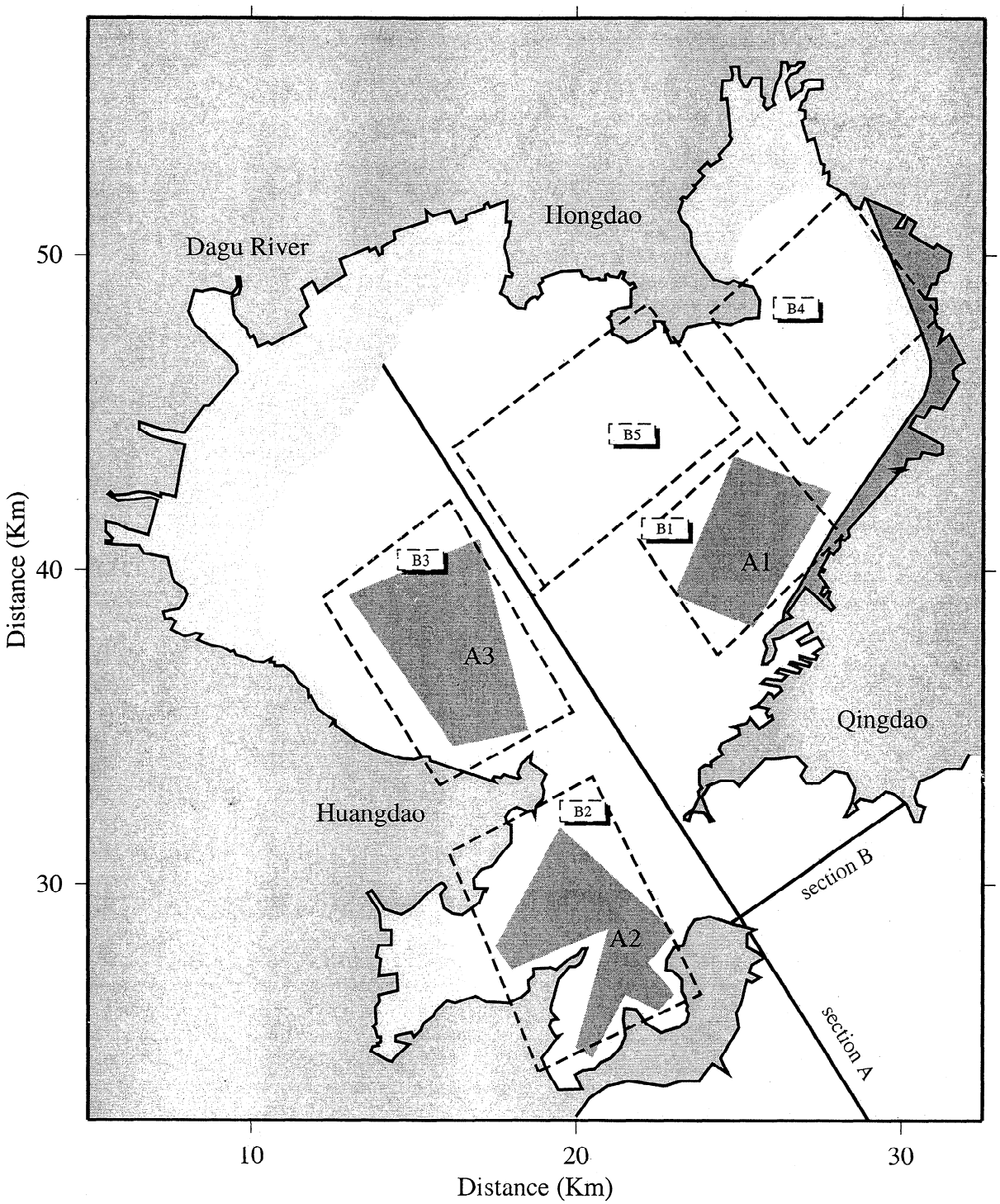

Figure 2. Locations of the shellfish aquaculture sites (shaded area) and selected regions for the flux estimation of nutrient and phytoplankton (areas enclosed by dashed line). The heavy solid lines indicate two sections used to represent our model results on cross-bay section (section A) and flux calculation into or out of the bay (section B).

water temperature and turbidity, and the amount of nutrients supplied from rivers, etc. The concentration of chlorophyll *a*, for example, has a range of 0.37 to 9.5 mg m^{-3}, with a peak occurring in summer [*Wu and Zhang*, 1995]. It is highest around the northwestern coast, where the Dagu River is located, and lowest near the entrance of the bay, where an anticyclonic residual eddy is found. Similarly, the primary productivity also varies widely and ranges from 33.60 to 2145.45 mg C m^{-2} d^{-1}, with the highest value near the northern coast in summer.

Shellfish aquaculture is prevalent in Jiaozhou Bay: the predominant species are suspended cultured scallops (local species *Chlamys farreri* and bay species *Argopecten irradians*) and bottom-cultured clams. Three popular regions for culturing scallops are indicated in Figure 2, an area which occupies 50 km^2, about 1/8 of the total area of the bay

[*Collaudin*, 1996]. The annual total production of aquacultured scallops is ~40,000 tons (fresh total weight), which makes it one of the leading sources of income for local seafood industries. *Ruditapes philippinarum* is the major aquacultured clam species in the intertidal and subtidal zones in the northern part of the bay. Approximately 77,000 tons (fresh total weight) are harvested annually.

The rapid growth of aquaculture, the unwise use of living marine resources, and the pronounced increase of nutrients and organic matter output from rivers in Jiaozhou Bay have caused a serious marine environmental problem. This is evidenced by the frequent occurrences of eutrophication and harmful algal blooms (so-called "red tide") and also by the rapid increase in mortality rates and decrease in growth rates of both natural and cultured marine organisms [*Collaudin*, 1996]. It is clear that the deterioration of the ecosystem in Jiaozhou Bay is caused by human activities. The dynamics that control this ecosystem, however, have not been well-understood. What are the impacts of river discharges, tidal mixing, current advection, and winds on the temporal and spatial variations of nutrients and hence on the phytoplankton in Jiaozhou Bay? Where is eutrophication most likely to occur? To what degree does aquacultured shellfish influence the ecosystem of the bay? Is the biological field mainly controlled by physical processes? What is the physical process controlling the material exchange between Jiaozhou Bay and the YS? To answer these questions, we must first understand the ecosystem dynamics associated with biological-physical interactions.

In this paper we examine the biological and physical processes that control the temporal variation and spatial distribution of nutrients and phytoplankton in Jiaozhou Bay using a modified simple coupled biological and physical model (originally developed by *Franks and Chen* [1996] and modified by *Chen et al.* [1997]). The physical model has provided a reasonable simulation of the amplitude and phase of the M_2 tide and residual circulation in Jiaozhou Bay. The coupled physical and biological model has revealed that in Jiaozhou Bay, nutrients (phosphates) were supplied and maintained directly by physical processes associated with tidal mixing, river discharges, residual current advection, and wind. The temporal and spatial distributions of phytoplankton were controlled dominantly by biological processes associated with nutrient uptake, grazing by zooplankton, and consumption by shellfish.

2. Coupled Physical and Biological Model

2.1. Physical Model

The physical model used in this study is a modified version of the three-dimensional (3-D) coastal ocean circulation model developed originally by *Blumberg and Mellor* [1987]. This model incorporates a free surface for tidal simulation and the *Mellor and Yamada* [1982] level 2.5 turbulence-closure scheme for parameters of vertical mixing. Time-variable river/dam and onshore intake/outflow discharges are included in the model for simulating the buoyancy flow caused by river discharges. The σ and curvilinear coordinate transformations are used in the vertical and horizontal direction, respectively, which allow a smooth representation of irregular bottom topography and coastal geometry. Physical forcings included in our numerical experiments were (1) an oscillating tide at the open boundary condition, (2) river discharges, and (3) winds. A detailed description of the updated version of this 3-D model is given by *Blumberg* [1994], *Chen and Beardsley* [1995], and *Chen et al.* [1999].

2.2. Biological Model

The biological model is developed by modifying a simple nutrient (N), phytoplankton (P), and zooplankton (Z) model [*Franks and Chen*, 1986]. The governing equations of this model are given as a form of

$$\frac{dP}{dt} = \frac{V_m N}{k_s + N} f(I_0) P - Z R_m (1 - e^{-\lambda P}) - \varepsilon P - S_F F_r P + \frac{\partial}{\partial z}(K_h \frac{\partial P}{\partial z}) \quad (1)$$

$$\frac{dZ}{dt} = \gamma Z R_m (1 - e^{-\lambda P}) - gZ + \frac{\partial}{\partial z}(K_h \frac{\partial Z}{\partial z}) \quad (2)$$

$$\frac{dN}{dt} = -\frac{V_m N}{k_s + N} f(I_o) P + (1-\gamma) Z R_m (1 - e^{-\lambda P}) + \varepsilon P + gZ + S_F \cdot E_r + \frac{\partial}{\partial z}(K_h \frac{\partial N}{\partial z}) \quad (3)$$

where V_m is the maximum phytoplankton growth rate, k_s is the half-saturation constant for phytoplankton growth, I_0 is the incident irradiance intensity, R_m is the maximum grazing rate of phytoplankton by zooplankton, λ is the grazing efficiency of phytoplankton by zooplankton, γ is the fraction of ingested phytoplankton unassimilated by zooplankton, g is the zooplankton death rate, ε is the phytoplankton death rate, K_H is the vertical diffusion coefficient for N, P, and Z, S_F is the stocking density of shellfish, F_r is the filtration rate of shellfish; and E_r is the excretion rate of shellfish. The derivative operator

$$\frac{d}{dt} = \frac{\partial}{\partial t} + u\frac{\partial}{\partial x} + v\frac{\partial}{\partial y} + w\frac{\partial}{\partial z}.$$

Aside from the inclusion of shellfish, the biological model is the same as that developed by *Franks and Chen* [1996] for Georges Bank, which presents a simple food web in which dissolved nutrients are taken up by phytoplankton following Michaelis-Menten kinetics and phytoplankton are grazed by zooplankton through an Ivlev functional response.

Some modifications to their original model have been made in our studies. First, unlike the nitrogen-limited system of Georges Bank, phosphate is the main nutrient that limits the growth of phytoplankton in Jiaozhou Bay. Therefore all parameters of nutrients, phytoplankton, and zooplankton used in our model were specified based on a phosphate-limited marine system.

Second, instead of using a constant mortality rate, we concurred with *Steele and Henderson* [1992] and *Kawamiya et al.* [1995] in assuming that ε is proportional to the biomass of P in a form of

$$\varepsilon = \delta P, \quad (4)$$

where δ is the new mortality rate that was assumed to be a constant value of 0.03 L μmol C^{-1} d^{-1} in our model. Numerical experiments have revealed that this mortality rate formula was robust to capture a conservative biological system under a condition without extra sources and sinks.

Third, we changed the formula of incident irradiance to make the diffuse attenuation coefficient dependent on water

depth. The dependence of the phytoplankton growth rate on incident irradiance intensity I_o was given as a form of

$$f(I_o) = I_o e^{-k_{ext} z} \tag{5}$$

where k_{ext} is the diffuse attenuation coefficient for irradiance. In Jiaozhou Bay the light penetration depth was found to vary significantly with water depth. It was <1 m at the 2-m isobath and ~5 m in the region deeper than 15 m [*Weng et al.*, 1992]. On the basis of these observed events we assumed that k_{ext} was given by

$$k_{ext} = \begin{cases} 1.4 - 0.08D & 0 < D \le 15\text{m} \\ 0.2 & D > 15\text{m} \end{cases} \tag{6}$$

Finally, we added shellfish (cultured shellfish) as a consumer of phytoplankton. The uptake rate of phytoplankton by shellfish is directly proportional to stocking density (S_F) and filtration rate (F_r). In general, S_F is known in the model since shellfish is an aquacultured species. F_r is affected by shellfish body weight, water salinity and temperature, and food concentration [*Winter*, 1978; *JØrgensen*, 1990]. All of these factors were determined by observation. In our model experiments, F_r was specified as a constant. Shellfish excretion contributes to the nutrient pool at a rate of. In general, E_r depends on the physiological condition of shellfish, the ambient water environment, and the available concentrations of food sources. For simplification, a constant value of E_r was used in our numerical experiment. This simplification satisfies our interest in understanding the impacts of aquaculture activities on the local- and bay-wide-scale ecosystem in Jiaozhou Bay.

2.3. Boundary and Initial Conditions

For a physical system driven only by tidal and wind forcings, the surface and bottom boundary conditions were given as

$$\left.\begin{aligned} &\frac{\partial T}{\partial z} = \frac{\partial S}{\partial z} = \frac{\partial P}{\partial z} = \frac{\partial Z}{\partial z} = \frac{\partial N}{\partial z} = 0 \\ &w = \frac{\partial \zeta}{\partial t} + u\frac{\partial \zeta}{\partial x} + v\frac{\partial \zeta}{\partial y} \\ &K_m\left(\frac{\partial u}{\partial z}, \frac{\partial v}{\partial z}\right) = (\tau_{sx}, \tau_{sy})/\rho \end{aligned}\right\} \quad z = \zeta(t, x, y) \tag{7}$$

and

$$\left.\begin{aligned} &\frac{\partial T}{\partial z} = \frac{\partial S}{\partial z} = \frac{\partial P}{\partial z} = \frac{\partial Z}{\partial z} = \frac{\partial N}{\partial z} = 0 \\ &w = -\left(u\frac{\partial H}{\partial x} + v\frac{\partial H}{\partial y}\right) \\ &K_m\left(\frac{\partial u}{\partial z}, \frac{\partial v}{\partial z}\right) = (\tau_{bx}, \tau_{by})/\rho \end{aligned}\right\} \quad z = -H(x, y) \tag{8}$$

where (τ_{sx}, τ_{sy}), and (τ_{bx}, τ_{sy}) are the x and y components of surface and bottom stresses, u, v and w are the x, y and z components of the water velocity, H is the mean water depth, ζ is the surface elevation, and K_m is vertical eddy viscosity.

The open boundary condition in the YS was specified by the oscillating surface elevation with amplitudes and phases of the observed M_2 tide. The tidal data were digitized directly from our East China Sea tidal model (note that the East China Sea model was developed at University of Georgia in 1997;

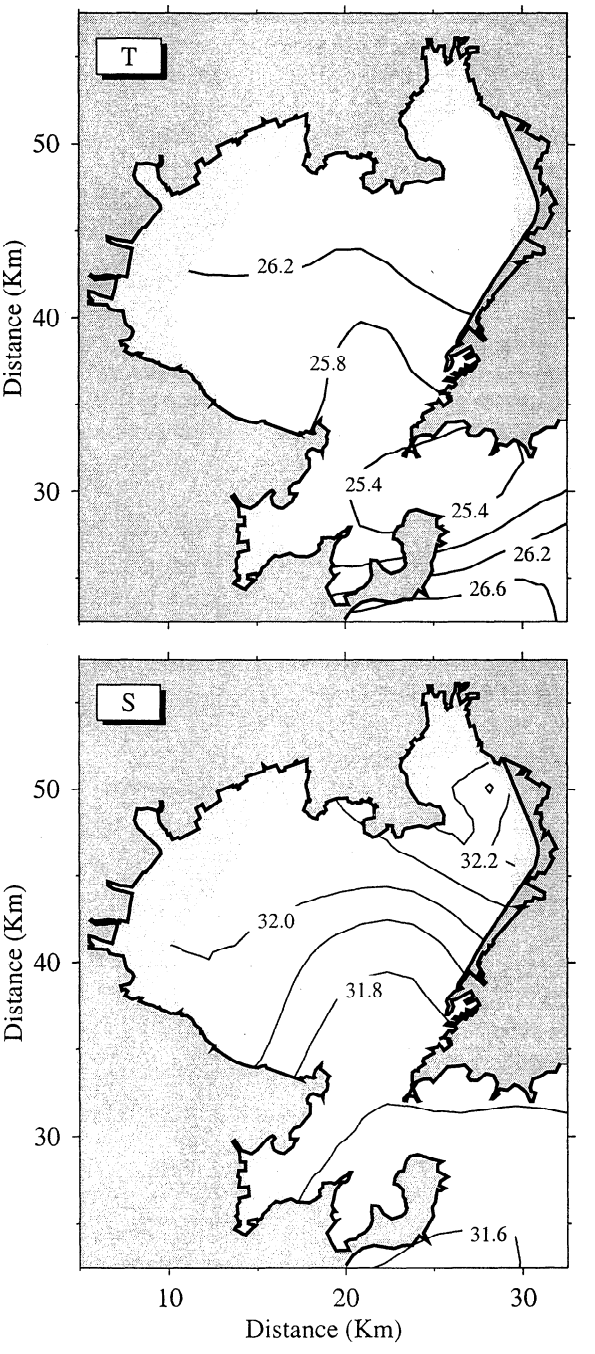

Figure 3. Initial distributions of temperature (°C) and salinity (PSU) of Jiaozhou Bay used in our model. The data were digitized directly from values of *Weng et al.*[1992].

the animation for the M_2 tidal simulation can be seen at (http://whale3.marsci.uga.edu/ research_projects/). Freshwater was injected into the model domain from the coastal boundary as a volume flux defined as

$$U_w = \Delta s \int_{-H}^{\zeta} u_w dz \tag{9}$$

where U_w is the velocity component normal to the coastline and Δs is the width of the river. The nutrient flux from a river was calculated as a product of the freshwater discharge rate and nutrient concentration at the mouth of a river.

Six rivers were included in our model experiments. They are the Dagu (largest one), Yang, Moshui, Baisha, Lichun, and Haibo Rivers. It should be noted here that our present model did not include the simulation of the intertidal zone in the northwestern part of the bay near the Dagu River. The real observations have shown that freshwater outflow from the Dagu River tended to occupy a relatively large region parallel to the boundary of the intertidal zone. To provide a more realistic distribution of freshwater discharges under a condition without inclusion of intertidal simulation, we have treated the Dagu River transport as a uniform flux band along the wet margin of the intertidal zone.

The initial distributions for temperature and salinity were specified using the climatological mean field in summer (Figure 3) [*Weng et al.*, 1992]. The initial distributions of biological state variables N, P, and Z were assumed to be vertically and horizontally homogenous in the numerical domain. This simplification was consistent with our assumption that all spatial and temporal variations in the biological field developed as a result of physical and biological interactions. The initial values of N, P, and Z were given based on the averaged values measured in early summer: they were 0.4 μmol P L^{-1}, 0.7 μg Chla L^{-1}, and 0.3 μmol C L^{-1}, respectively.

2.4. Biological Parameters

The biological parameters used in our model experiments are listed in Table 1. Since these parameters varied in a wide range with time and space, we first ran the model with an initial setup of parameters and then carried out a sensitivity analysis over parameter ranges. A detailed description of our initial setup of biological parameters is given below.

The maximum phytoplankton growth rate V_m is a species-specific and temperature-dependent parameter. Based on *Skeletonema sp.* and *Nitzschia sp.*, the most dominant species in Jiaozhou Bay during summer [*Guo and Yang*, 1992], this value ranges from 1.0 to 2.0 at a temperature of 20°C. A mean value of 1.5 was chosen for our model experiments. Half saturation constant k_s for phytoplankton also is a species-specific parameter and varies in a range of 0.09 to 1.72 μmol P L^{-1} [*JØrgensen et al.*, 1991; *Valiela*, 1995]. A relatively high value of 0.3 μmol P L^{-1} was used for our model, in consideration of the eutrophication of the coastal water in Jiaozhou Bay and the nutrient concentration outside the bay.

Table 1. Parameters for the Biological Model

Parameter	Description	Value
V_m	maximum phytoplankton growth rate, d^{-1}	1.5
K_s	half-saturation constant for phosphate uptake, μmol P L^{-1}	0.3
R_m	zooplankton maximum grazing rate, d^{-1}	0.6
γ	assimilated fraction by zooplankton	0.4
λ	Ivlev constant for grazing, L μmol C^{-1}	0.25
δ	dependence of phytoplankton mortality rate, L d^{-1} μmol C^{-1}	0.03
g	zooplankton mortality rate, d^{-1}	0.2
C/P	atomic ratio of carbon and phosphate	100
C/Chl *a*	weight ratio of carbon and chlorophyll *a*	60
C/DW	weight ratio of carbon and zooplankton dry weight	0.35
S_F	standing stock of cultured scallop, individuals L^{-1}	0.012
F_r	filtration rate of scallop, L d^{-1} individual^{-1}	100
E_r	excretion fraction of filtrated food	0.3

There were few measurements for the maximum zooplankton grazing rate R_m and grazing efficiency of phytoplankton by zooplankton λ in Jiaozhou Bay. Some studies on the ingestion of phytoplankton by zooplankton were carried out using a gut fluorescence method [*Li*, 1997], but no data have been provided for R_m and λ. In general, R_m and λ depend on species and size of zooplankton and phytoplankton. They vary in ranges of 0.16 to 1.5 d^{-1} and 0.01 to 0.35 μmole C L^{-1} in the coastal water, respectively [*McAllister*, 1970; *Franks et al.*, 1986; *Kremer and Nixon*, 1978]. The constant values of R_m= 0.6 d^{-1} and λ = 0.25 μmole C L^{-1} were used initially in our model.

The assimilated fraction of phytoplankton by zooplankton γ varies in a range of 0.2 to 0.7, with a majority between 0.3 and 0.4 in the marine system [*Raymont*, 1980; *Franks et al.*, 1986]. For our model, γ was chosen as 0.4, which represented an unassimilated efficiency of 60%. The zooplankton death rate g is an uncertain parameter in modeling experiments. A wide range of 0.07 to 1.75 d^{-1} has been used previously [*Steele*, 1974; *Steele and Henderson* 1981; *Franks et al.* 1986; *Franks and Chen* 1996; *Chen et al.*, 1997]. A constant value of g = 0.2 d^{-1} was used in our model experiments, which was the same as that used by *Franks et al.* [1986].

The stocking density of shellfish S_F was calculated directly from in situ measurements taken in Jiaozhou Bay in 1996 [*Collaudin*, 1996]. The aquaculture area was determined precisely by using a Global Positioning Satellite (GPS), and the stocking data were counted based on numbers of lanterns and individuals per lantern. S_F was set to 12 individuals m^{-3} (= 0.012 individuals L^{-1}) in our experiments. This value was obtained based on an averaged number of three cultured areas. The recent physiological measurements taken in Jiaozhou Bay show that F_r varies in a range of 30 to 200 L d^{-1} individual^{-1}) around a temperature of 25°C in summer. These filtration rates may be overestimated since no food concentration was taken into account [*Winter*, 1978]. For this reason, a value of F_r = 100 L d^{-1} individual^{-1} was used in our model, which should present an average filtration rate (after taking the food concentration into account) in Jiaozhou Bay in summer. In addition, E_r was taken as 0.3 in our model, which represented 30% of the ingested food.

As mentioned above, the *NPZ* model of Jiaozhou Bay described a phosphorus-limited ecosystem. In our model experiments, phytoplankton and zooplankton were measured in units of carbon and nutrients by units of phosphorous. A constant C/P atomic ratio of 100 was used to convert the carbon to phosphorous. The C/Chl *a* ratio also was used to convert chlorophyll *a* to carbon. This ratio in general varies from 20 to 145 for different species and at different measurement sites [*JØrgenson et al.*, 1991]. The recent measurements of POC and chlorophyll-a in Jiaozhou Bay suggested a higher C/Chl *a* ratio of 60 in this region [*Yang and Liu*, 1995; *Wu and Zhang*, 1995], which was 2 times larger than the value of 30 suggested by *Kremer and Nixon* [1978]. We used 60 as the C/Chl *a* ratio in our studies.

2.5. Design of Numerical Experiments

The model domain (see Figure 4) covers the entire area of Jiaozhou Bay and has an open boundary on the western coast of the YS. The shaded regions shown in Figure 2 are the intertidal zones which have not been included in our numerical computation even though they were covered by model grids (note that the model boundary was at the outer

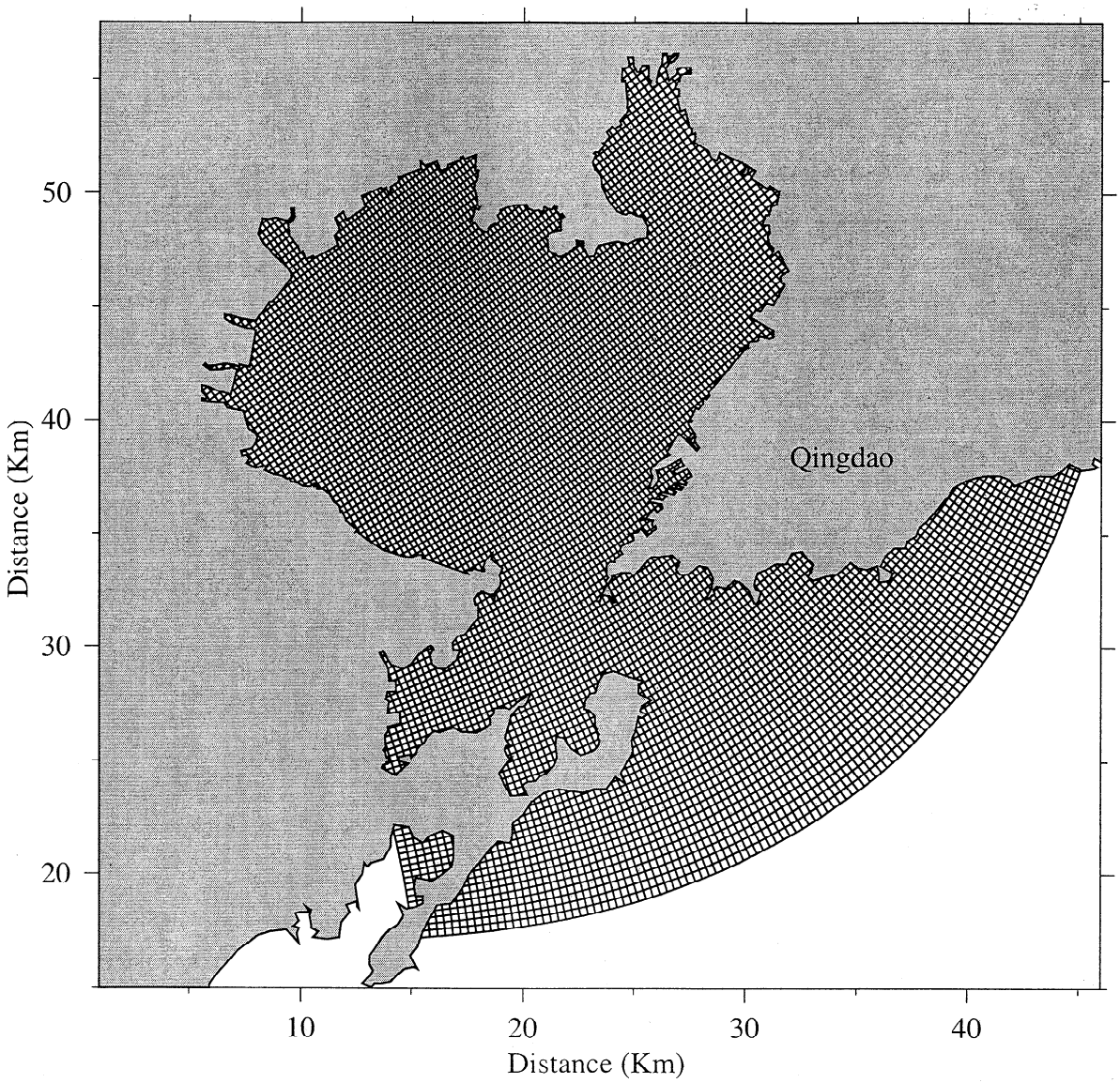

Figure 4. Horizontal numerical grids of Jiaozhou Bay. Horizontal resolution is 200 m with a total cells of 119×114.

edge of the intertidal zone). The horizontal grids were designed using an orthogonal curvilinear coordinate transformation with total cells of 119 ×114. The horizontal resolution was about 200 m. The 11 σ levels were used in the vertical, which provided a vertical resolution of ~0.3 m near the coast and ~5 m outside the bay where the water depth was ~50 m.

The model ran prognostically as an initial value problem forced by an oscillating surface elevation with amplitudes and phases of the observed M_2 tide at the open boundary. After the tide reached an equilibrium state, six rivers were then added to the numerical domain. The freshwater discharge rate and nutrient concentration of each river are shown in Table 2. These were obtained from measurements taken in 1991 [*Liu and Wang*, 1992]. We also have examined the influences of wind-induced currents and mixing on the temporal variation and spatial distribution of temperature, salinity, nutrients, and phytoplankton. For simplification, a constant southeasterly wind of 5 m s^{-1} was added into the model after 10 model days. The time step used in the numerical computation was 103.5 s, which corresponded to 432 steps for a M_2 tidal cycle.

Table 2. River Discharge to Jiaozhou Bay in Summer 1991

River	Rate of discharge, $m^3 s^{-1}$
Dagu	87.42
Yang	6.36
Moshui	3.66
Baisha	2.38
Lichun	0.60
Haibo	0.40

The seasonal average was made based on the data shown by *Liu and Wang* [1992].

3. Model Results

3.1. Tidal Simulation

The M_2 tidal elevation and current reached an equilibrium state after 5 model days. The coamplitude and cophase of the model-predicted M_2 tidal elevation are shown in Figure 5. The model results showed that the tide propagated into the bay from the YS and then turned clockwise as it traveled toward the northern coast. The amplitude of the tide was ~120 cm at

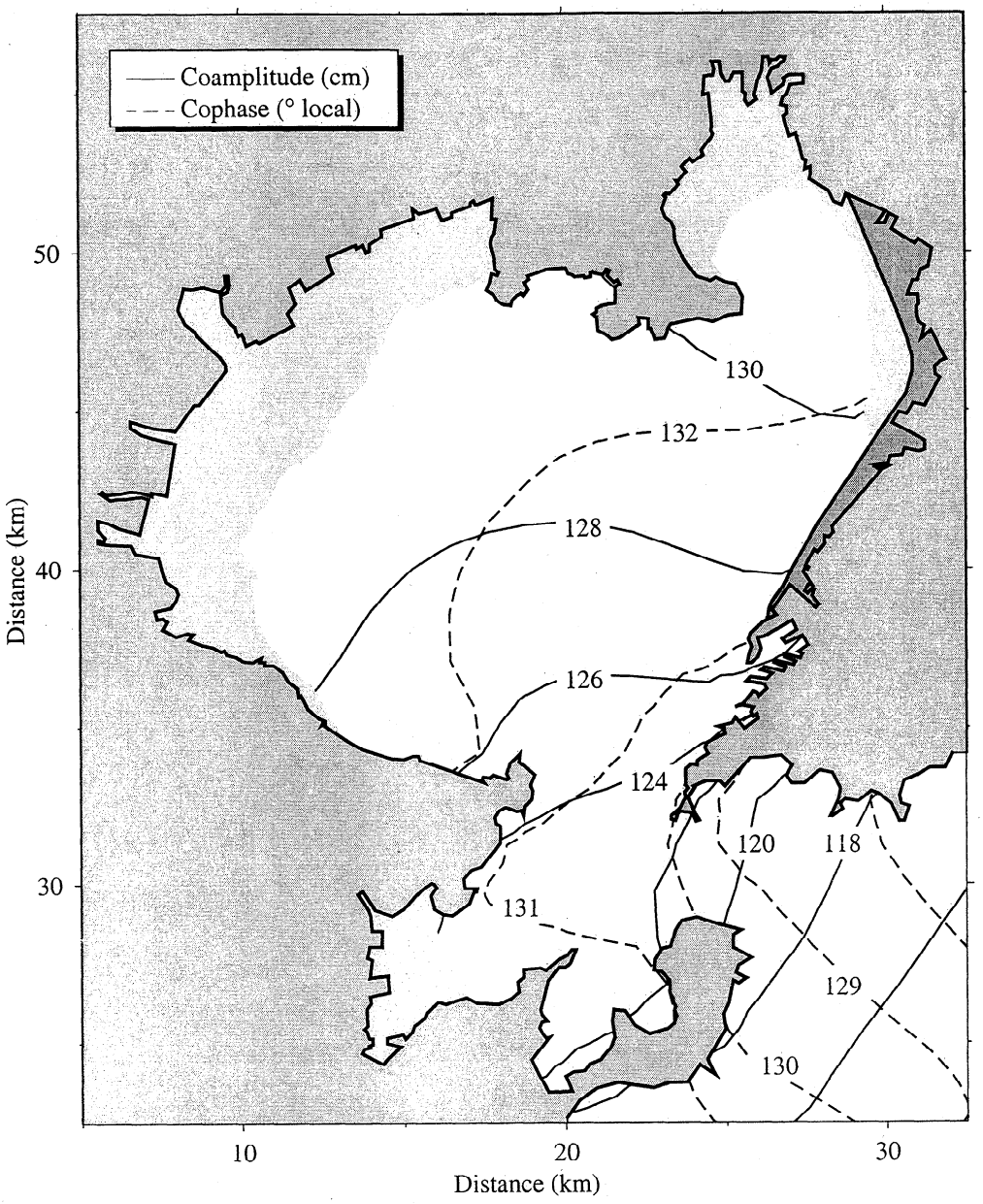

Figure 5. Computed coamplitudes (cm) and cophases (degrees local) of the semidiurnal M_2 tidal constituent in Jiaozhou Bay.

the entrance of the bay and reached a maximum of about ~130 cm near the northeast coast. The maximum phase difference inside and outside the bay was about 3°. It took only 6.2 min for the tidal peak to travel from the YS to the northern coast of the bay. There were only two tidal gauge stations around Jiaozhou Bay available for our purposes: one was at Dagang and the other was at Dashitou (see Figure 1). The amplitudes and phases of the model-predicted M_2 tide were in good agreement with observational data available at these two tidal stations. The differences of computed and observed amplitudes and phases were 0.2 cm and 1.9° at Dagang and 1.4 cm and 1.1° at Dashitou (Table 3).

Figure 6 shows synoptic distributions of computed M_2 tidal current vectors over a tidal cycle with a time interval of ~3 hours. The water flushed northward into the bay and in turn drained out the bay during flood and ebb tides. The maximum speed of the surface tidal current was ~40 cm s^{-1} inside the bay and larger than 70 cm s^{-1} in the strait connected to the YS. At the transition from flood to ebb tide (high tide), the tidal current in the bay was mainly characterized by a relatively weak, clockwise circulation. This circulation, however, disappeared at the tidal transition from ebb to flood, indicating an asymmetric tidal current over a tidal cycle. This asymmetric feature also was evident in the strait during flood and ebb tides. At the maximum flood tide, due to inertial

Table 3. Comparison Between the Observed and Computed Amplitude and Phase of M_2 Tidal Constituent in Jiaozhou Bay

Stations	Amplitude (cm)		Phase (° local)	
	Obsserved	Computed	Observed	Computed
Dagang	126.4	126.2	132.8	130.9
Dashitou	125.3	123.9	131.9	130.8

Locations of Dagang and Dashitou are indicated in Figure 1.

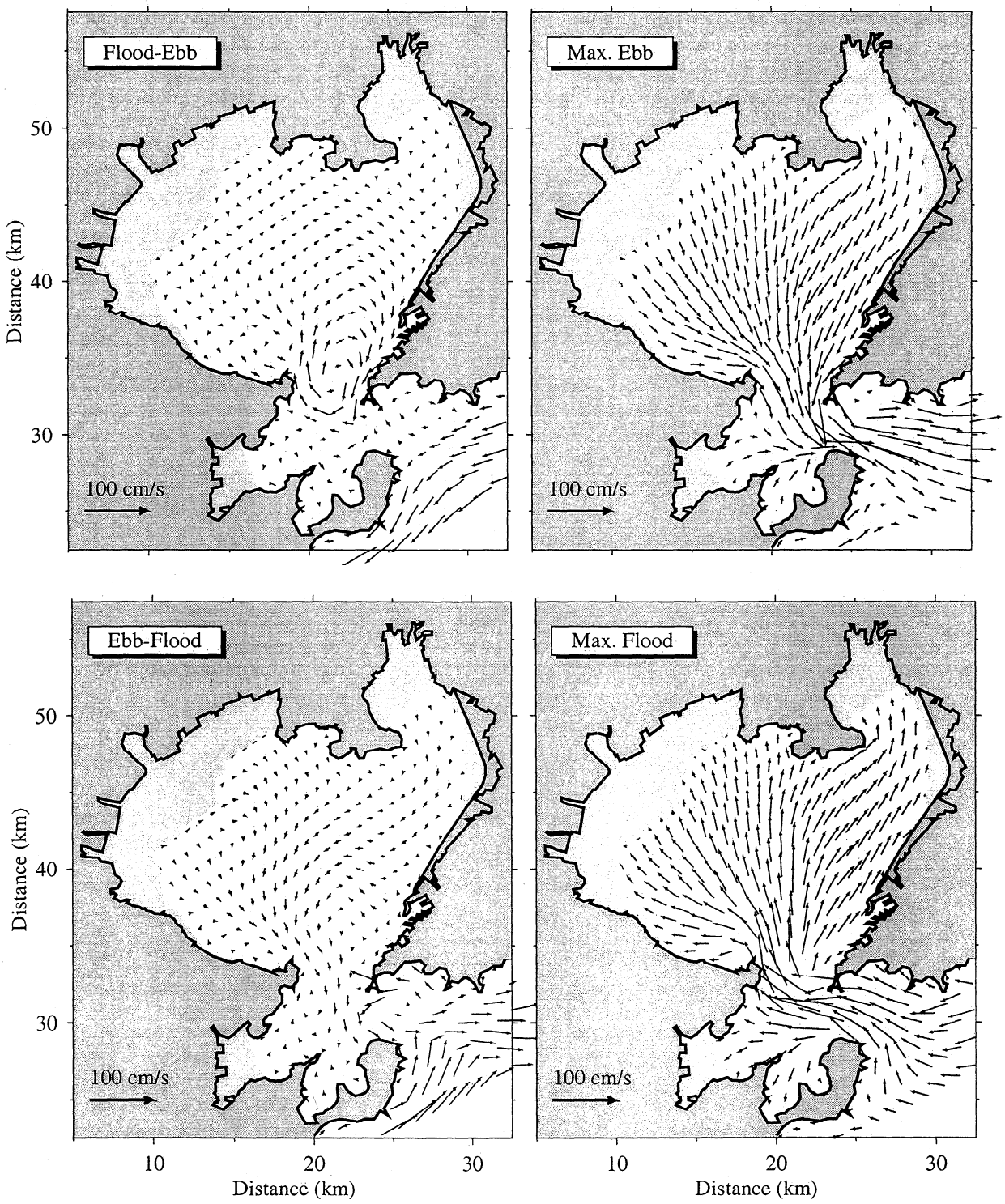

Figure 6. Synoptic distributions of the surface tidal current vectors of the M_2 tide at the times of flood to ebb, the maximum ebb, ebb to flood, and maximum flood.

effects, the water flushed into the bay with a larger transport at the left side of the strait near Dashitou. Conversely, at the maximum ebb tide, it moved out of the bay with a larger transport on the right side of the strait near Dagang.

Our model results of the M_2 tidal simulation also were consistent with previous work done with a 2-D (vertically averaged) model [e.g., *Weng et al.*, 1992]. Unlike previous models, the 3-D model used in this study had fine horizontal and vertical grids and provided a more precise tidal simulation for Jiaozhou Bay. Resolving the vertical structure of the motion was important for the study of the ecosystem in this region since most of our interest in a coupled biological and physical system was in the eutrophic zone near the surface.

3.2. Residual Circulation

The asymmetric feature of tidal current over a tidal cycle resulted in strong clockwise residual eddy circulation in the southern part of Jiaozhou Bay between Dashitou and Dagang. This relatively strong eddy-like clockwise residual current was believed to be caused by local geometrical coastline and bottom topography. The velocity of this residual eddy circulation was about 15 to 20 cm s^{-1} (Figure 7a), with a vertically averaged velocity of about 10 to 15 cm s^{-1} (Figure 7b). In most regions of Jaiozhou Bay, where the water depth was <10 m, the residual current was characterized by a weak clockwise circulation near the surface which was relatively stronger on the eastern side than on the western side. Vertically averaged residual currents in these shallow regions were very weak, <0.2 cm s^{-1} on the western side and ~1.5-2.5 cm s^{-1} on the eastern side.

The residual circulation pattern was not significantly modified in the case with river discharges and an initial setup of temperature and salinity (Figures 7c and 7d). River discharges slightly enhanced the clockwise residual current near the northwestern and eastern coasts. The current tended to flow across the density contours from coast to the inner bay. (Note that to make our description and discussion easier and clearer, we divided Jiaozhou Bay into two regions: inner and outer bays. The inner bay is defined as a region where the water depth is shallower than 5 m, and the rest of the area is defined as the outer bay.)

The response of the residual current to wind varied with water depth. For example, in the case with a southeasterly wind of 5 m s^{-1}, the near-surface water in the shallower region of <10 m tended to move northwestward in a direction of the wind, while the wind did not significantly alter the residual eddy circulation in the strait between Dashitou and Dagang (Figure 7e). Vertically averaged residual circulation in the case with wind was very similar to that in the case with only tide and river discharges, suggesting that wind did not change water transport in Jiaozhou Bay much, although it significantly modified the vertical profile of residual current (Figure 7f). A weak clockwise residual circulation was found in the northwest region of the bay in the case with wind, which was believed due to wind and tidal interactions. The wind caused a near-surface convergence toward the northwest region of the bay, which enhanced vertical mixing and hence enforced tidal rectification in that region.

The physical mechanism responsible for the generation of residual flow in Jiaozhou Bay differed considerably from that over Georges Bank and in the inner shelf of the South Atlantic Bight where the motion also is dominated by the M_2 tide [*Chen et al.*, 1995; *Chen and Beardsley*, 1998; *Chen et al.*, 1999]. On Georges Bank, for example, the residual current is mainly driven by the convergence and divergence of the cross-isobath momentum flux against bottom friction [*Loder*, 1980, *Chen and Beardsley*, 1995, *Chen et al.*, 1995]. In this case, the tidally rectified current always flows along local isobaths with a shallower region to the right. In Jiaozhou Bay the weak clockwise residual circulation found in the shallower region of the bay was caused by bottom friction. However, the residual eddy circulation near the entrance of the bay formed due to an asymmetric water movement through the narrow strait during flood and ebb tides, which had nothing to do with bottom friction.

3.3. Tidal Cycle Average Distributions of T, S, N, and P

The model results show that the water temperature remains vertically well-mixed throughout Jiaozhou Bay except in the deeper regions where a slight decrease in temperature from surface to bottom was found (Plates. 1a and 2a). Surface water temperature increased northward across the bay and ranged from 25.9° C at the entrance of the bay to as much as 26.2° C in the inner bay (Plates 1a). A tongue-like band of colder water was found in the outer bay between Dashitou and Dagang and appeared to be connected to the cold water source in the YS [*Chen et al.*, 1994]. The temperature contours are almost parallel to the local isobath with a maximum gradient at the outer edge of the tongue-like cold water band.

Similarly, the model-predicted salinity also remained vertically well-mixed throughout the entire bay except in the deeper region near the southern entrance (Plates. 1b and 2b). The surface salinity decreased northward and had values of 32 in the southern region near Dagang and Dashitou and 29 along the wet margin of the intertidal zone in the northwestern region. A front with relatively low salinity formed near the coast in the northwestern area of the inner bay. It was mainly caused by output from the Dagu River. The model-predicted location and intensity of the salinity front were in good agreement with observed data [*Weng et al.*, 1992].

The observations show that the water in the northwest coastal region of Jiaozhou Bay, which is originally injected from the Dagu River, generally has a higher salinity [*Weng et al.*, 1992] than that which was predicted by our model. This contrast was not surprising since our present model did not include the intertidal zone. In summer, considerable evaporation occurs in the intertidal zone due to high temperature and drying of water during the ebb tide. Substantial salt deposits near the surface in that area are dissolved into the water and carried back to the bay by either river output or by tidal flushing. One can easily take this effect into account by running the model with a river discharge source that has a higher salinity. However, since the model-predicted location and intensity of the salinity or density front were not changed by this effect, the present model results for salinity met our main interests in understanding coupled biological and physical processes.

The spatial distributions of nutrients (phosphate) and phytoplankton cohered well with the fields of salinity and temperature (Plates 1c and 1d). Similar to distributions of temperature and salinity, the nutrients and phytoplankton in Jiaozhou Bay remained well-mixed in the vertical (Plates 2c and 2d). The concentrations of nutrients and phytoplankton were highest in the coastal area of the inner bay and decreased dramatically toward the outer bay (Plates 1c and 1d). The maximum values of nutrients and phytoplankton were 1.65 μmol P L^{-1} and 1.9 μg Chl *a* L^{-1} near river sources in the inner bay, respectively, while they dropped to 0.42 μmol P L^{-1} and 0.8 μg Chl *a* L^{-1} near the southern entrance. In Jiaozhou Bay the lowest concentrations of nutrients and phytoplankton were found in the strait between Dashitou and Dagang, which coincided with the tongue-like cold water band found in that area of the bay.

No distributions of model-predicted zooplankton are shown here. One of the reasons is that there are very few observational data of zooplankton available for Jiaozhou Bay [*Gao and Yang*, 1995], nor do we have any data for model

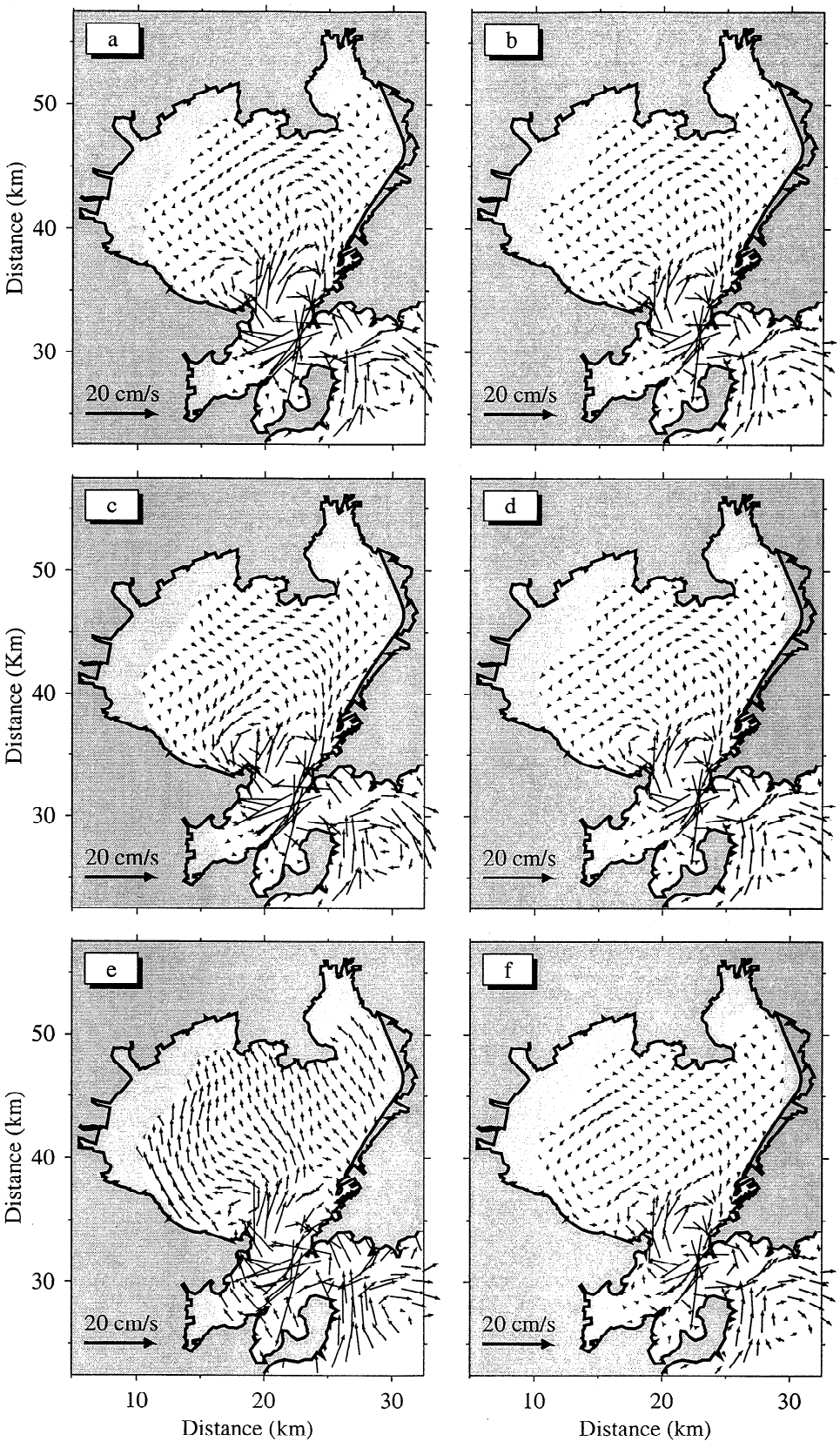

Figure 7. Distributions of the (left) surface and (right) vertically-averaged residual current vectors averaged over a tidal cycle at the end of the 5th day for the cases with (a, b) only tidal forcing, (c, d) tide plus freshwater discharges, and (e, f) tide plus freshwater discharges and wind (a southeasterly wind of 5 m s^{-1}). In the case with tide only, the initial temperature and salinity were specified as constant everywhere, while in the other two cases, the initial distributions of temperature and salinity were given using the climatological mean field in summer.

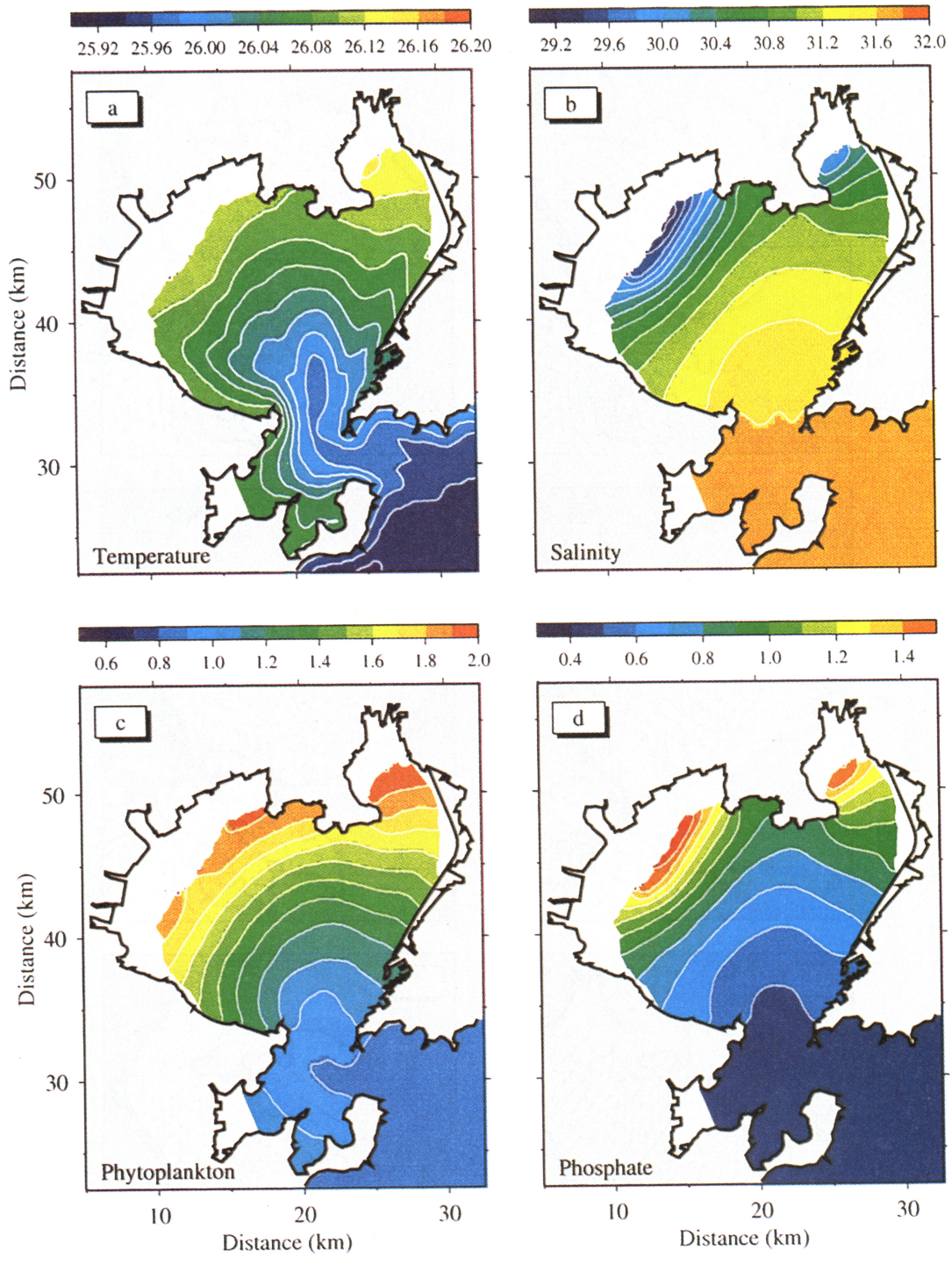

Plate 1. Tidal averaged surface distributions of (a) temperature (°C), (b) salinity (PSU), (c) phytoplankton (μg Chl *a* L^{-1}), and (d) phosphate (μmol P L^{-1}) at the end of the 20 model days for the case with only tide and freshwater discharges.

and data comparison. To shorten the manuscript, we have eliminated it in our discussion here. (Note that an animation of model-predicted zooplankton in Jiaozhou Bay can be viewed at Chen's web site.)

3.4. Effects of the Southeasterly Wind

As described above, the southeasterly wind tended to advect the near-surface water northwestward in the shallower region of the bay where the water depth was <10 m (Figure 7). The wind-induced northwestward advection and mixing slightly increased the temperature gradient around the 5-m isobath in the inner bay and cooled the tongue-like water band near the entrance of the bay (Plate 3a). A similar response also was found in salinity, where the salinity contours in the southwestern area of the bay were slightly pushed northward due to wind (Plate 3b). Wind mixing tended to cause both water temperature and salinity to remain well-mixed in the

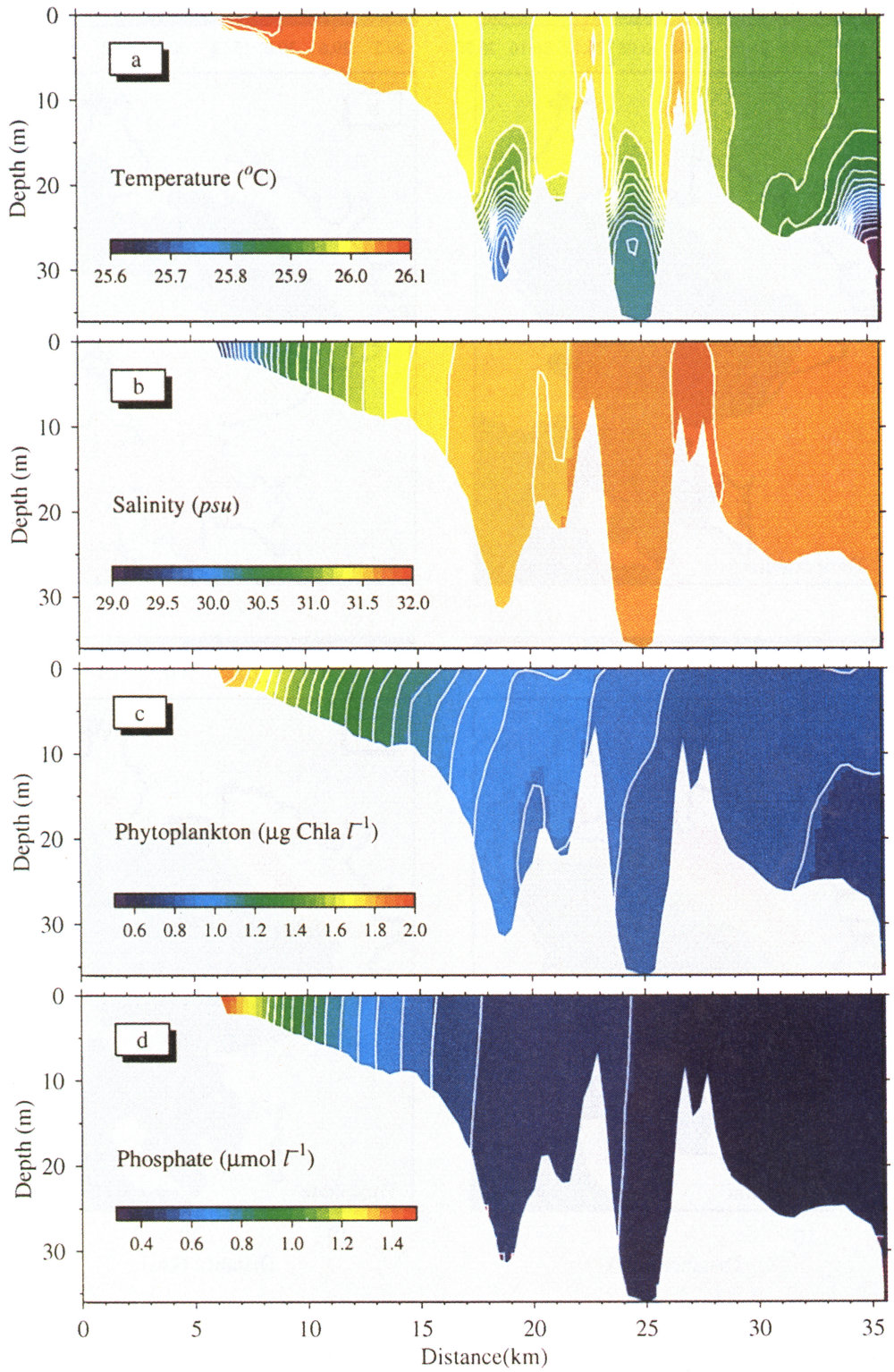

Plate 2. Tidal averaged vertical distributions of (a) temperature (°C), (b) salinity (PSU), (c) phytoplankton (μg Chl *a* L^{-1}), and (d) phosphate (μmol P L^{-1}) on section A (Figure 2) at the end of the 20 model days for the case with only tide and freshwater discharges.

vertical, even though the residual currents near the surface and bottom flowed in the opposite direction (Plate 4).

The wind exhibited a direct impact on the spatial distributions of nutrients in the inner bay. The wind pushed nutrients northward, leading to a high "accumulation" of nutrients in the innermost region near the northern coast. This resulted in a growth of phytoplankton in that area. Nutrient values were very similar to that of salinity in both the horizontal and vertical, suggesting a physically controlled ecosystem in Jiaozhou Bay (Plates 3 and 4).

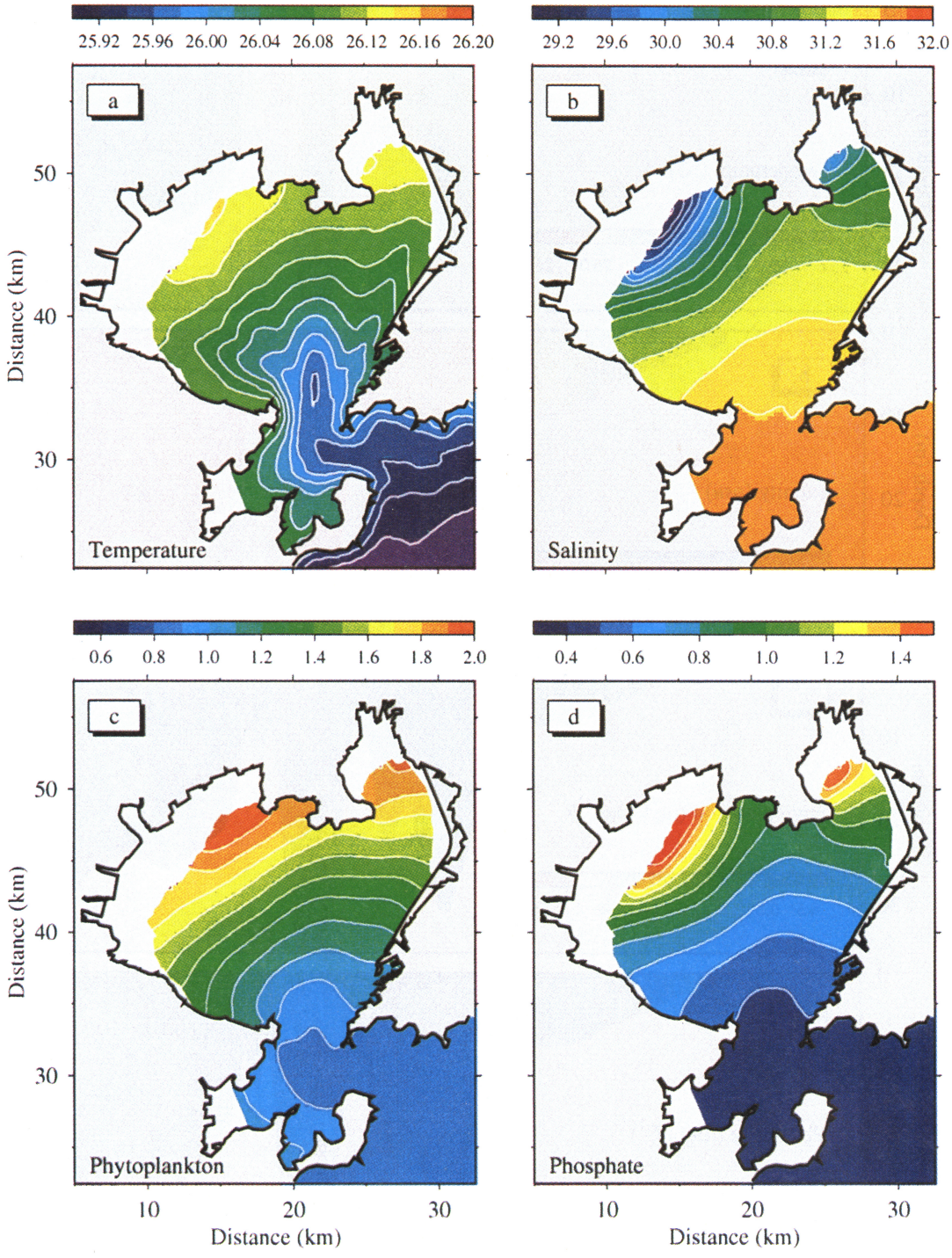

Plate 3. Tidal averaged surface distribution of (a) temperature (°C), (b) salinity (psu), (c) phytoplankton (μg Chl *a* L^{-1}), and (d) phosphate (μmol P L^{-1}) at the 20 model days for the case with tide, freshwater discharge, and a southeasterly wind (5 m s^{-1}).

3.5. Effects of Aquaculture Activities

Numerical experiments have been made for two different sets of shellfish stocking density with the same filtration and excretion rates. The shellfish terms in the model were introduced after 10 model days when the field of phytoplankton reached almost an equilibrium state in the case with river discharges and tidal and wind forcings. Shellfish stocking density (scallop) S_F was set to 12 indviduals m^{-3} (=0.012 individuals L^{-1}) in the first case, and it was doubled in the second case. Scallops grazing in cultured areas dramatically decreased the local concentration of phytoplankton. It dropped to 0.99 μg Chl *a* L^{-1} in A1, 0.52 μg Chl *a* L^{-1} in A2, and 1.0 μg Chl *a* L^{-1} in A3, about 31.8%, 33.3%, and 37.3% lower than those in the case without shellfish, respectively (Plate 5a). The response of phytoplankton to shellfish stocking density was not linear.

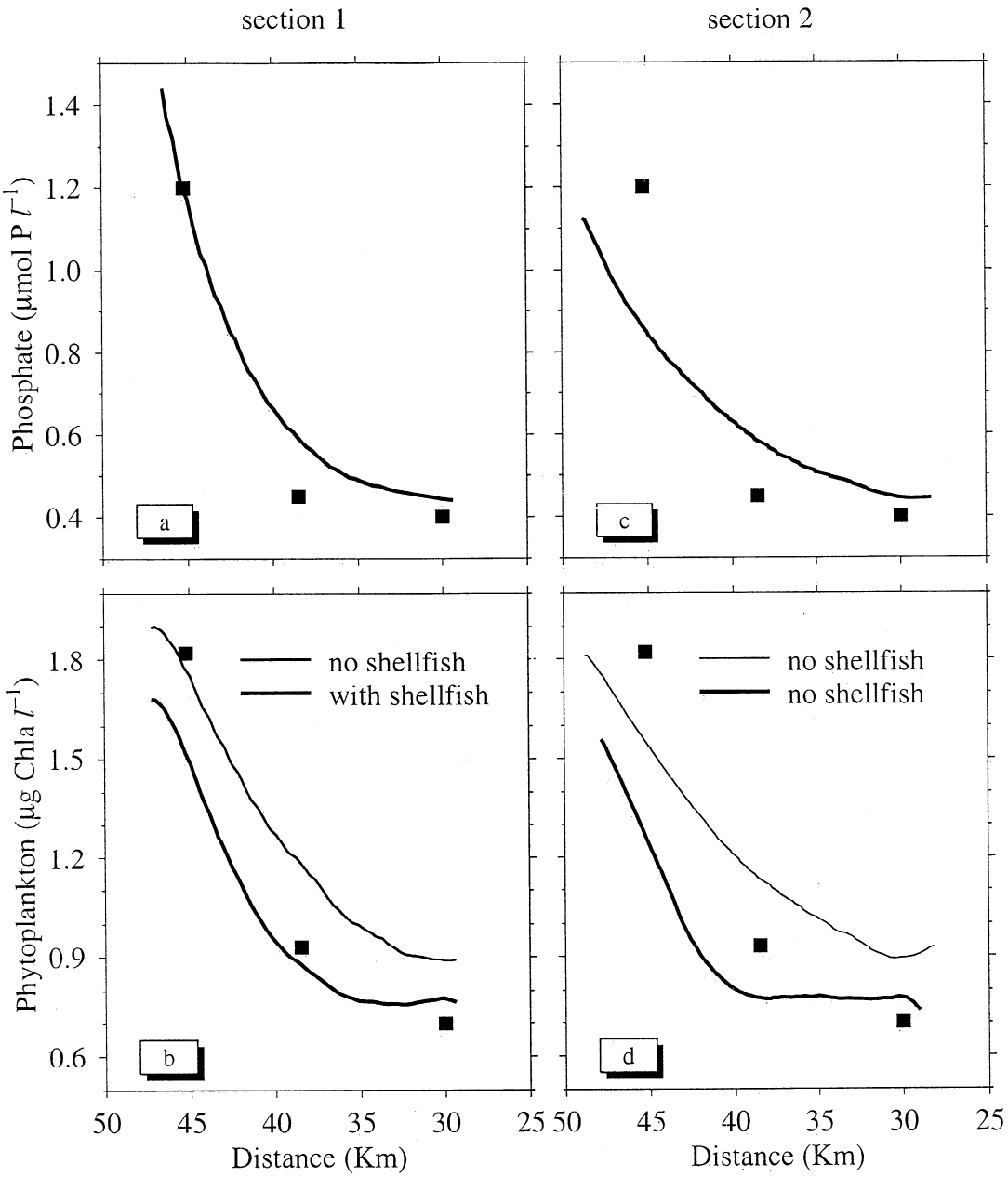

Figure 8. Comparisons between model-predicted and observed phosphates and phytoplanktons on sections 1 and 2. The solid squares indicate the observed values. The model-predicted values are presented by the thin (for the case with no shellfish) and heavy (with shellfish) solid lines. Note that the difference in phosphate between two cases (with and without shellfish) cannot be distinguished from the plot, so we have only plotted the phosphate for the case without shellfish.

When S_F was doubled in cultured areas (= 24 indviduals m^{-3}), the concentration of phytoplankton dropped to 0.71 μg Chl *a* L^{-1} in A1, 0.38 μg Chl *a* L^{-1} in A2, and 0.67 μg Chl *a* L^{-1} in A3: they were ~51.1%, 50.8%, and 55.6% lower than in the case without shellfish, but only ~19%, 18%, and 22% in the case with a shellfish stocking density of 12 indviduals m^{-3} (Plate 5b).

The impact of scallop culture on the concentration of nutrients seemed very small, even in the case with a high shellfish stocking density. This finding is in contrast with some other previous studies, which showed shellfish as having an important role in nutrient cycling and spatial distribution [Dame, 1993]. A possible explanation is that our present model did not take the biodeposition process of shellfish into account. This process allowed shellfish to take up small particulate organic matter and hence to produce feces and pseudo-feces, which can decompose into inorganic nutrients. Our model did include the scallop excretion, which was directly converted to phosphate. If the above explanation was valid, we should be able to see a significant modification of the nutrient concentration when we increased either excretion rate or stocking density of shellfish. However, we found that was not the case in our numerical experiments. Another possible reason was that most of the phosphate in Jiaozhou Bay was a result of loading from the land and rivers. The recycling of nutrients via shellfish may directly influence

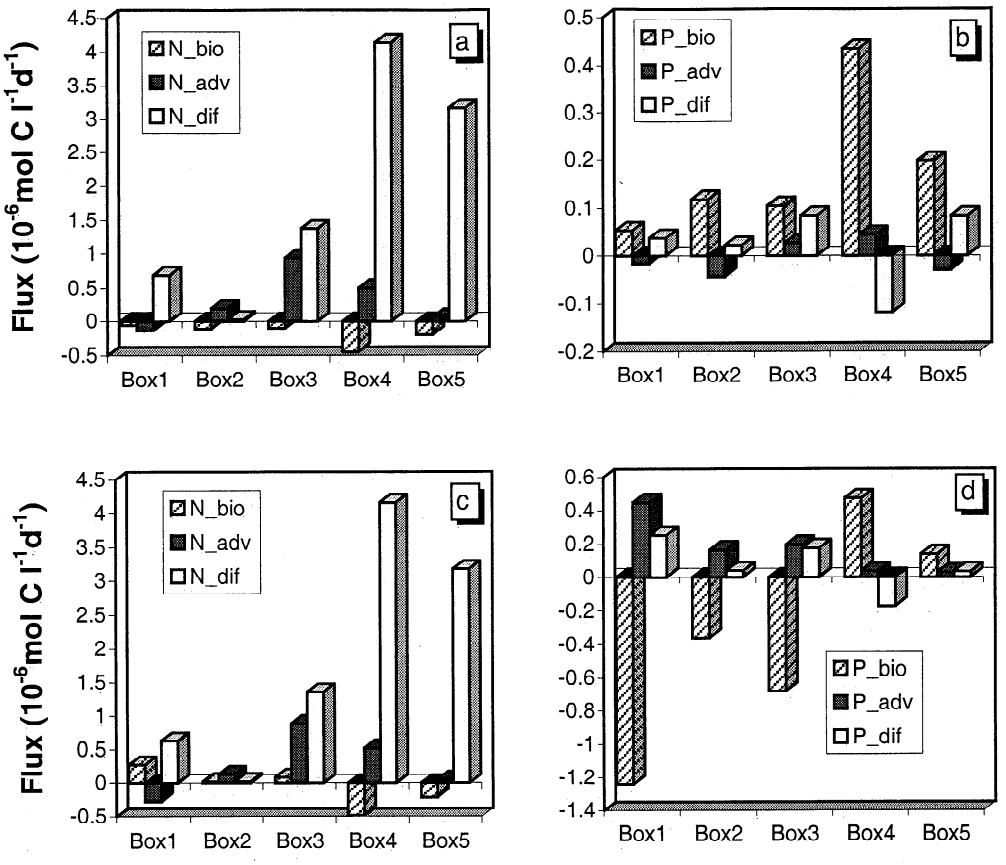

Figure 9. Net fluxes of nutrient (*N*, μmol P d^{-1}) and phytoplankton (*P*, g Chl *a* d^{-1}) into selected five regions (shown in Figure 2) for the cases (a, b) without and (c, d) with shellfish. The positive value indicates the flux into the box.. The tags of bio, adv, and dif indicate the fluxes caused by biological processes, advection, and diffusion, respectively.

the concentration of nitrogen but not of phosphates, or the nutrient regeneration rate may be orders of magnitude smaller than the nutrient loading rate from land and rivers. All these questions should be addressed in future observations.

3.6. Nutrients Uptake and Regeneration

To understand the roles of biological proccsses in the maintenance of the phosphate-limited ecosystem of Jiaozhou Bay, we have examined the nutrient uptake and regeneration processes in our coupled biological and physical model. The nutrient uptake in our modified *NPZ* model was defined by the first term on the right side of the phytoplankton equation (equation (1)), which was controlled by the phytoplankton growth rate, the incident irradiance, the half-saturation constant, the phytoplankton biomass, and the nutrient concentration. Nutrient regeneration was estimated by the sum of zooplankton excretion, death of phytopalnkton and zooplankton, and shellfish excretion on the right side of the nutrient equation (equation (3)).

In the case with only tides and freshwater discharges the model showed that the surface distributions of the uptake and regeneration rates were very similar to the distribution of nutrients, which decreased from the inner bay to the outer bay with highest values around the northwestern and northern coasts (Plates 6a and 6b). The maximum regeneration rate in the inner bay was ~2 μmol C L^{-1} d^{-1}, which was ~5 times smaller than the maximum uptake rate there. This suggests that the physical process associated with river discharges was a major source for the supply of nutrients for phytoplankton in the inner Jaiozhou Bay.

Adding a southeasterly wind did not significantly change the spatial distributions of nutrient uptake and regeneration (Plates 6d and 6e). A relatively large nutrient uptake rate was found in the innermost bay around the coast and was a result of the "accumulation" of nutrients caused by the wind-induced northwestward advection. This may explain why a phytoplankton bloom was favored to occur in the innermost bay during a southeasterly wind.

When the consumption of phytoplankton by shellfish was included in our food web, the spatial distributions of nutrient uptake and regeneration were remarkably modified, especially in the aquaculture sites (Plate 6g and 6h). The nutrient uptake rate in three aquaculture sites dramatically decreased due to a loss of phytoplankton. On the other hand, the nutrient regeneration rate in these sites increased substantially as a result of shellfish metabolism. The distribution of nutrients (phosphate) was almost the same in the case with and without shellfish aquaculture, suggesting that the decrease in the nutrient uptake rate due to the consumption of phytoplankton by shellfish was almost compensated for by physical processes associated with advection and diffusion (see detailed discussion in section 4).

We also have estimated the f ratio using the model-predicted nutrient uptake and regeneration rates. The f ratio is defined as a ratio of new production to total production. In our model the new production was equal to the difference between nutrient uptake and regeneration rates, and the total production was estimated by the nutrient uptake rate [*Franks and Chen*, 1996; *Chen et al.*, 1997]. The distribution of f ratio was high in the inner bay and low in the outer bay. In the case with only tide and river discharges, it varied from 0.4 to 0.9 in the inner bay (Plate 6c). Adding the wind did not significantly change the distribution of the f ratio (Plate 6f). This ratio changed noticeably when the consumption of phytoplankton by shellfish was included (Plate 6i). This was consistent with our previous finding that the decrease in the nutrient uptake rate was almost compensated for by physical processes.

It should be pointed out that the model-predicted f ratio was larger than that observed in the inner Jiaozhou Bay [*Wang et al.*, 1995]. This was probably because the definition of the f ratio used in our model differed from that used in observations. In general, both new and total productions are estimated by including ammonia that is generated in the biological system itself. In Jiaozhou Bay, most of the ammonia measured in the water comes from river discharges or land loading. The failure to distinguish the source of the ammonia in the measurement may cause an overestimate of the f ratio in the bay.

3.7. Comparison With Observations

A pilot field measurement of biological variables (phosphate and chlorophyll *a*) was made at five sampling stations in Jiaozhou Bay in August 1996 (see Figure 1). A comparison between model-predicted and observed phosphate and chlorophyll *a* was conducted on cross-bay sections 1 and 2 (shown in Figure 1). Regardless of whether or not wind or shellfish aquaculture was included, the distributions of model-predicted nutrients did not change much, and all were in good agreement with observations (Figure 8a). In the case with only tide and river discharges, the concentration of model-predicted phytoplankton was a little higher than that observed in the outer bay (Figure 8b). Adding the shellfish aquaculture tended to reduce the concentration of phytoplankton. This agreed closely with observations in the interior bay but underestimated the phytoplankton concentration in the inner bay. Similar spatial distributions of phosphate and chlorophyll *a* also were found during summer in previous measurements in Jiaozhou Bay [*Wu and Zhang*, 1995], which supported our model predictions. In addition, since the five measurement sites were distributed spatially over the bay, a good agreement between the distributions of model-predicted and observed nutrients and phytoplankton at these sites suggested that our model results, to certain extent, were robust.

It should be noted that the model and data comparison seemed more meaningful qualitatively than quantitatively, since no error bars were provided in the measurements. More intense interdisciplinary measurements are needed to verify our model findings quantitatively. It also was one of the reasons why we focused our model experiments more on process studies than on simulation.

4. Fluxes of Nutrients and Phytoplankton

One of our main interests here is to identify, qualify, and quantify the roles of physical and biological processes in the maintenance of the marine ecosystem in Jiaozhou Bay. In the simple *NPZ* food web system, the physical processes included (1) advection and (2) diffusion. Biological processes referred to the terms on the right side in equations (1)-(3). For example, the biological processes in the phytoplankton equation (equation (2)) referred to nutrient uptake, phytoplankton grazing and mortality, and shellfish consumption. In the nutrient equation (equation (3)) the biological processes referred to the nutrient regeneration and nutrient uptake by phytoplankton. To examine the effects of freshwater discharge and shellfish aquaculture on the local ecosystem in the bay, we have estimated the net flux of nutrients and phytoplankton into or out of five closed regions and across the outer strait at the entrance of the bay (see section B in Figure 2). The flux was calculated based on tidally averaged values over the 10 tidal cycles. We understood that no steady state probably could be reached over the time period we were interested. When we say "equilibrium state" here, we mean that the flux is balanced for a first-order approximation in which the biological field would still change slowly with time for an order of magnitude smaller. Since our main interests here are to find out the dominant process attributed to the major change of nutrients and phytoplankton, we think our flux analysis meets our need.

In the case that did not take the shellfish aquaculture into account, the supply of nutrients in sites 1, 4, and 5 was mainly supported by nutrient diffusion. Both advection and diffusion controlled nutrients in site 3, which was close to the largest river source (Figure 9a). In site 2, which was located in the southwestern corner of the outer bay near Huangdao, the nutrients were mainly supplied by advection from the surrounding area. The model also shows a relatively large nutrient flux out to the YS by advection. This suggested that Jiaozhou Bay acted as a main nutrient source for the YS ecosystem. In this case, the biological processes seemed to play a minor role in the maintenance of nutrients in all five sites.

Unlike the nutrient flux, the maintenance of phytoplankton in sites 2, 4 and 5 was mainly controlled by biological processes associated with nutrient uptakes and phytoplankton

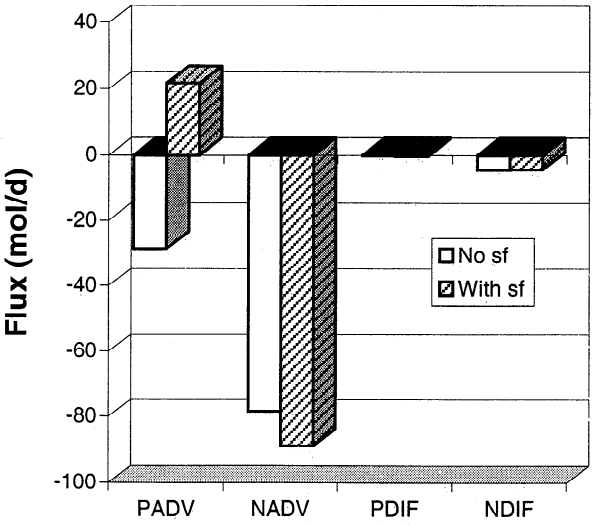

Figure 10. Net fluxes of phytoplankton (g Chl *a* d^{-1}) and phosphate (mol P d^{-1}) across section B caused by advection and diffusion. ADV and DIF incicate advection and diffusion.

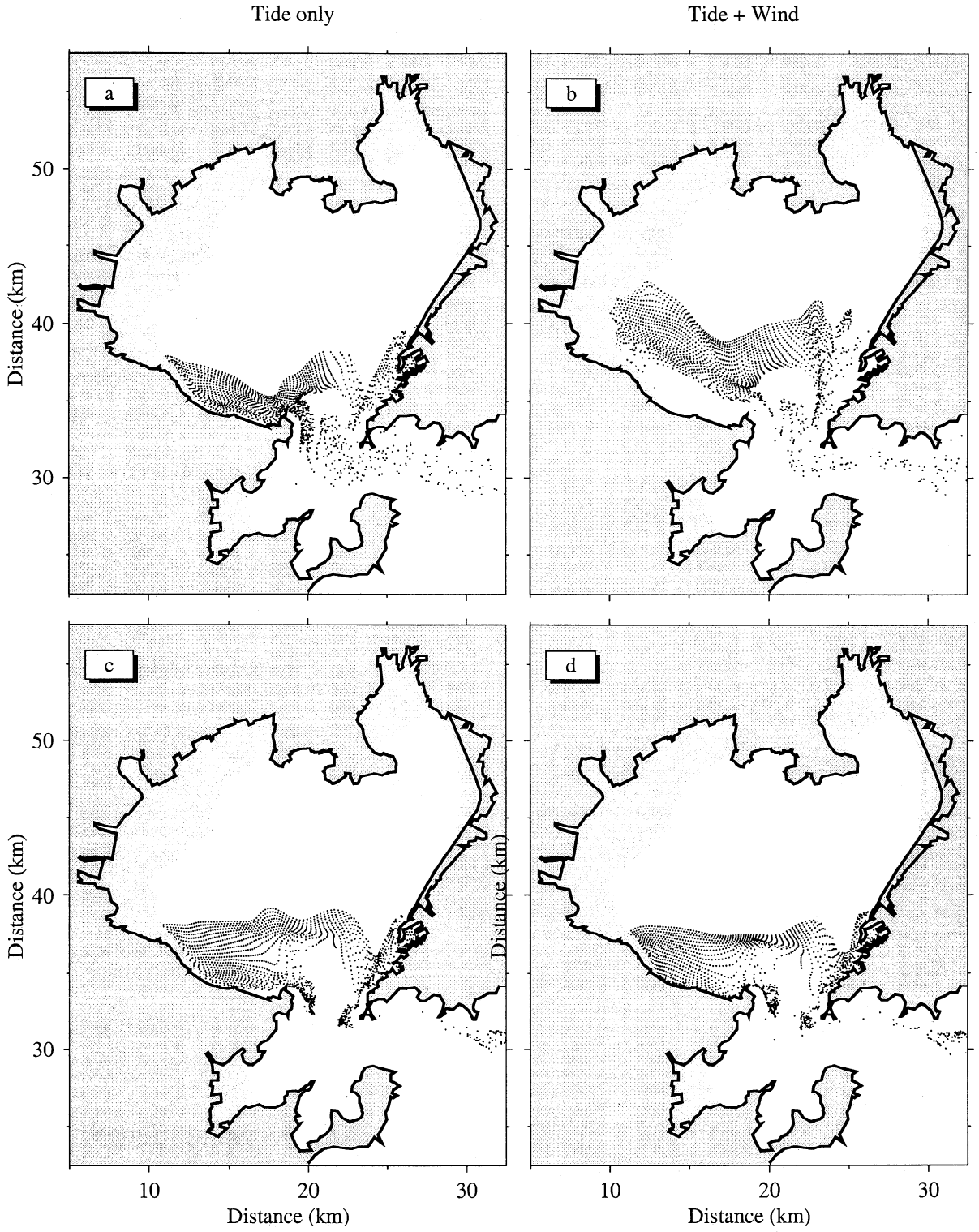

Figure 11. The distributions of particles at the end of the second tidal cycle after they deployed for the case with (a,c) tide only and (b,d) tide plus wind. The particles were initially deployed at the surface and near-bottom at the 10th model day (see Figure 1).

grazing (Figure 9b). In site 3 near the largest river source, both advection and biological processes were almost equally important. The advection also tended to advect the phytoplankton out of Jiaozhou Bay into the YS (Figure 10).

Shellfish aquaculture did not change the mechanism for the maintenance of nutrients and phytoplankton in Jiaozhou Bay. The nutrients in all five sites were still supplied by physical processes associated with horizontal diffusion and advection (which was only important near river sources). Phytoplankton was controlled dominantly by biological processes. However, the inclusion of shellfish aquaculture did change the flux to the YS. The large consumption of phytoplankton by shellfish

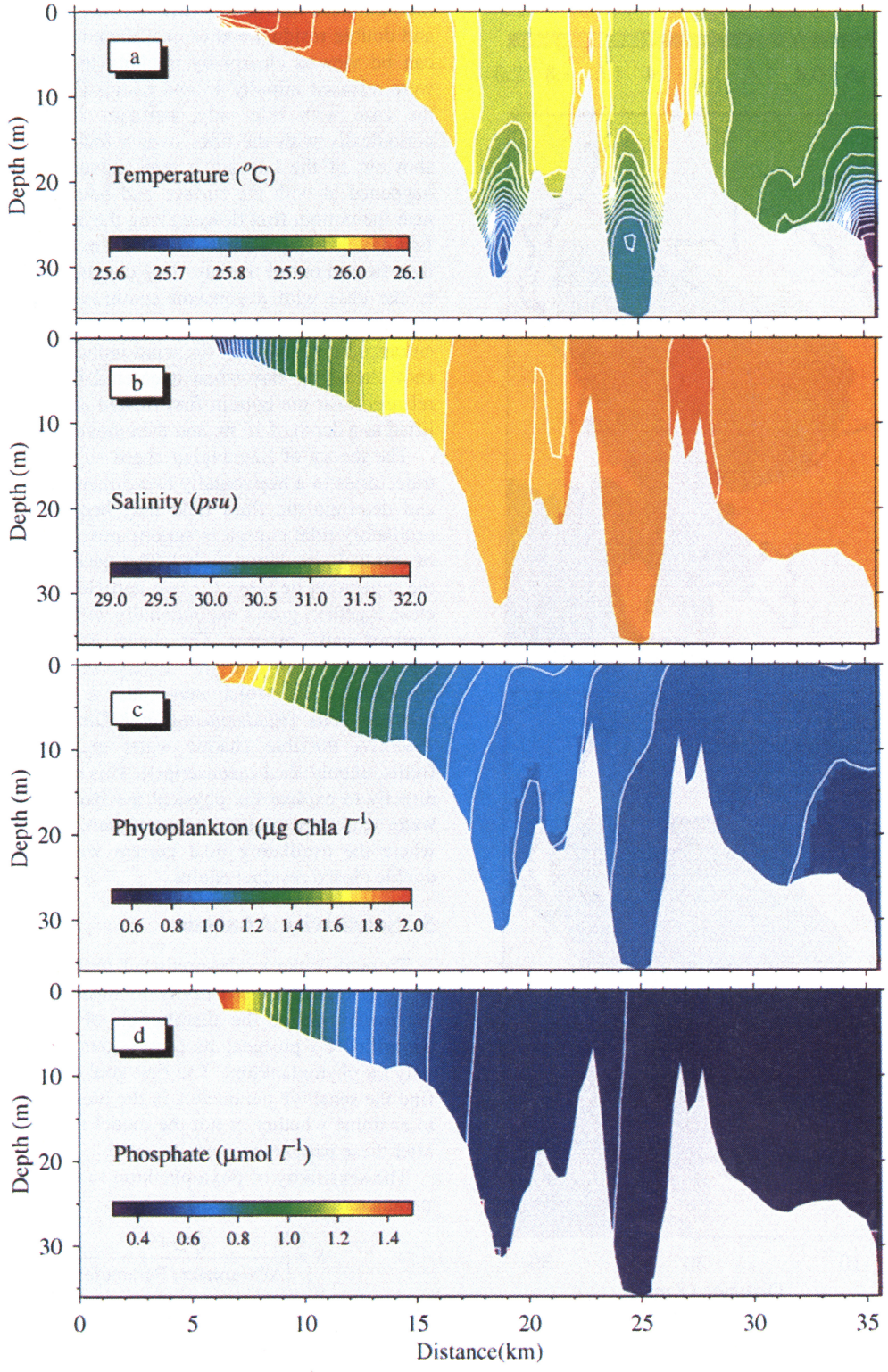

Plate 4. Tidal averaged vertical distribution of (a) temperature (°C), (b) salinity (PSU), (c) phytoplankton (µg Chl *a* L^{-1}), and (d) phosphate (µmol P L^{-1}) on section A (Figure 2) at the 20 model days for the case with tide, freshwater discharge, and a southeasterly wind (5 m s^{-1}).

caused a net flux into the bay from the YS, even though nutrients still tended to be advected out of the bay (Figure 10). The loss of phytoplankton in the shellfish aquaculture sites also was compensated for by the flux advected or diffused from the surrounding water, which tended to modify the entire ecosystem of Jiaozhou Bay.

To examine the water exchange between Jiaozhou Bay and the YS, we released passive fluid particles at the surface (σ = 0) and near the bottom (σ = 10) in the northern region of the bay entrance, respectively. At each of these two σ levels a total of 2014 particles were deployed at the end of the 10th model day and traced for 5 days. For the case with tide only, a

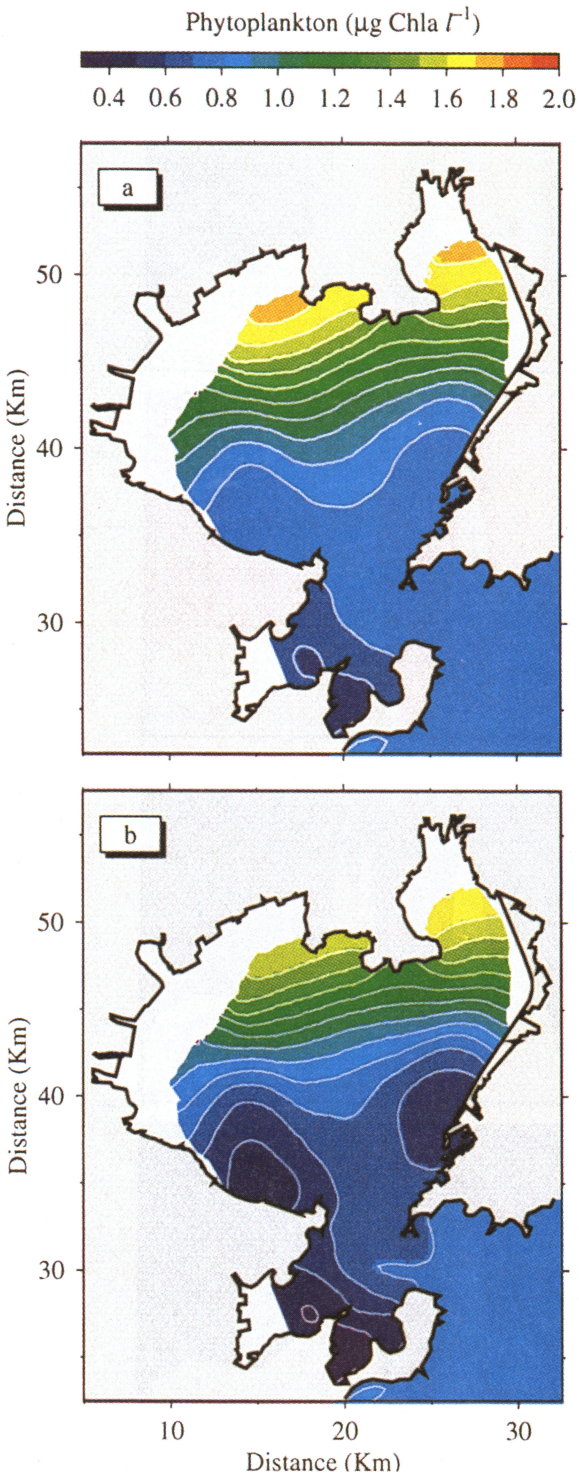

Plate 5. Tidal-cycle averaged surface distribution of phytoplankton at the 20 model days for the case with the shellfish culture densities of (a) 12 and (b) 24 individuals m^{-3}. Physical forcings are the same as that shown in Plate 4.

large amount of particles at the surface and near the bottom moved through the strait and entered the YS (Figures 11a and 11c). Although a constant southeasterly wind advected parts of near-surface particles to move northwestward, a significant amount of near-surface particles still flowed out of Jiaozhou Bay (Figure 11b and 11d).

The particle exchange between Jiaozhou Bay and the YS was controlled by a chaotic kinematic process associated with the nonlinear interaction between periodical tidal oscillation and double residual eddies near the entrance of the bay. This can be viewed clearly by tracking individual particles that were released initially around eddies (Figures 12 and 13). In the case with tide only, particles near eddies oscillated periodically with the tides over a few tidal cycles and then shot out of the bay when they moved into the strait. This happened at both the surface and bottom. Particles released near the bottom first flowed along the bottom slope during the first day, lifted to a depth of about 5 m below the surface, and then flowed out of the bay. This chaotic feature also occurred in the case with a constant southeasterly wind. A particle released at the surface around the eastern coast near the entrance moved against the wind-induced surface current and shot out of the bay when it entered the strait. The particle released near the bottom first flowed along the bottom slope, lifted to a depth of 15 m, and then moved out of the bay.

The theory of Lagrangian chaos suggests that the particle trajectories in a horizontally two-dimensional, incompressible and deterministic fluid field may become chaotic when an oscillatory tidal current is superimposed upon a regular array of residual circulation cells [*Zimmerman*, 1986]. As a result, the separation between the two particles, which initially were close together, grows exponentially with time through a "tidal random walk" process. The chaotic stirring may occur near the saddle point at the transverse intersection of the circulation cells, which may cause a rapid water exchange between cells [*Ridderinkhof and Zimmerman* 1992; *Chen, 1999* (A possible chaotic water exchange across coastal fronts, unpublished manuscript)]. This concept can be applied directly to explain the physical mechanism for the kinematic water exchange process between Jiaozhou Bay and the YS, where the oscillating tidal current was superimposed upon double closed residual eddies.

5. Sensitivity Analysis

To qualify the model-predicted biological fields, we have tested the model's sensitivity to uncertainties in biological parameters. Since the distribution of nutrients was mainly controlled by physical processes, our analysis was focused only on phytoplankton. The first goal of this analysis was to find the sensitive parameters in the biological model and then to examine whether or not the model results were still robust after these parameters were changed.

The sensitivity of phytoplankton to variations in biological parameters was estimated here by

$$\hat{S} = \left| \frac{\Delta P / P}{\Delta \text{Parameter} / \text{Parameter}} \right| \tag{10}$$

where $\hat{S}$ is a measure of sensitivity, P is the concentration of phytoplankton in the model run with standard biological parameters (listed in Table 1), and ΔP is the change of P caused by varying the model parameter. ΔParameter is varied by 1% from the standard value.

The sensitivity of phytoplankton to changes in biological parameters is shown in Table 4. The analysis results showed that S at five measurement sites was smaller than 0.5 for most of the biological parameters used in the model except for V_m (the maximum phytoplankton growth rate). A value of ~1 was found for V_m, suggesting that it was the most sensitive parameter in the biological model. We have rerun the model with V_m =1.0 and 2.0 d^{-1}, 0.5 smaller or larger than its standard value. The model results show that the basic pattern of the

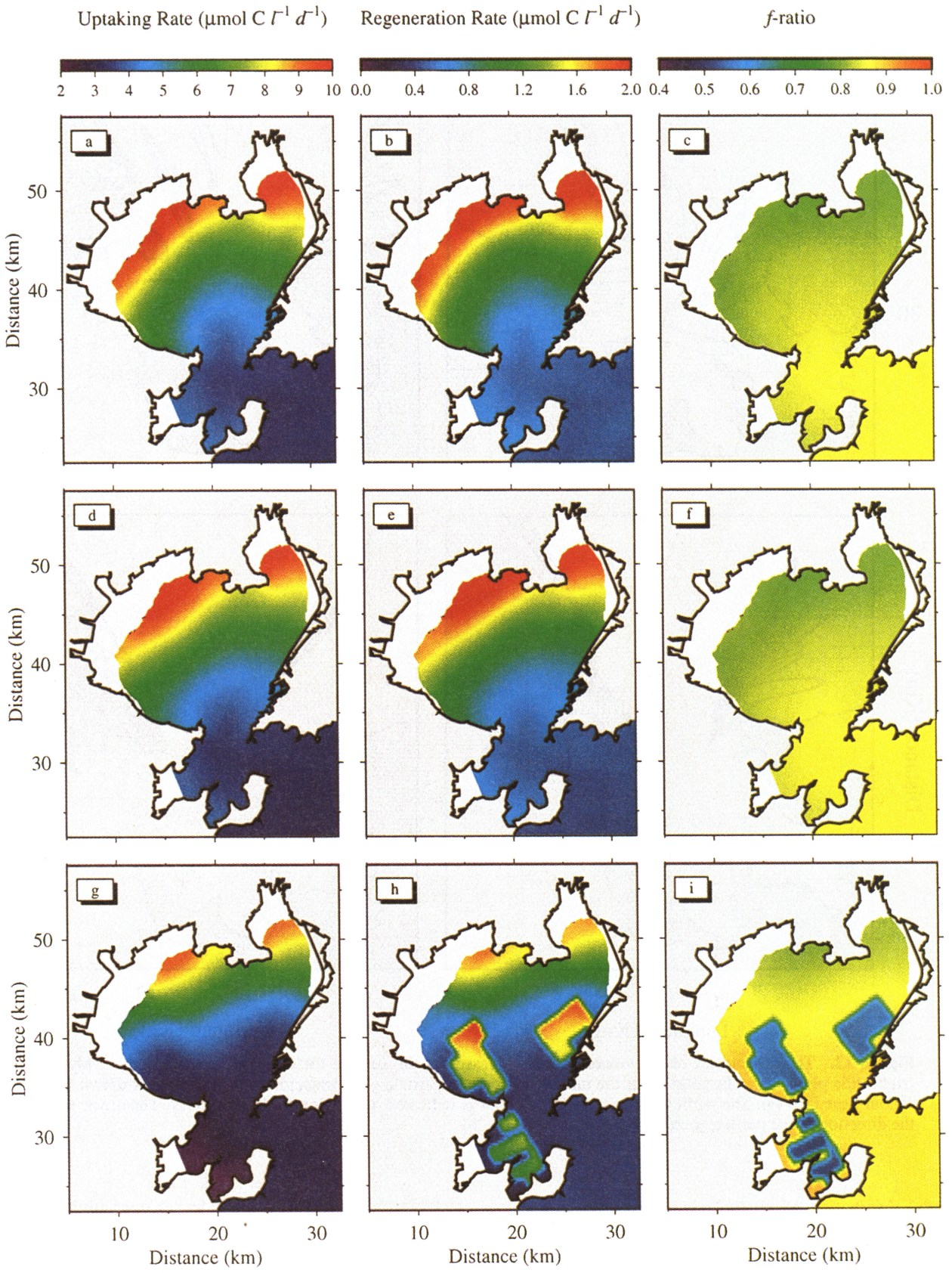

Plate 6. Tidal-cycle averaged distributions of uptake rate, regeneration rate, and *f* ratio in Jiaozhou Bay for the cases with (*a, b, c*) tide plus river discharges, (*d,e,f*) tide plus river discharges and wind, and (*g,h,i*) tide plus river discharges and wind as well as shellfishes. The shellfish stocking density in this case is 12 individuals.m^{-3}.

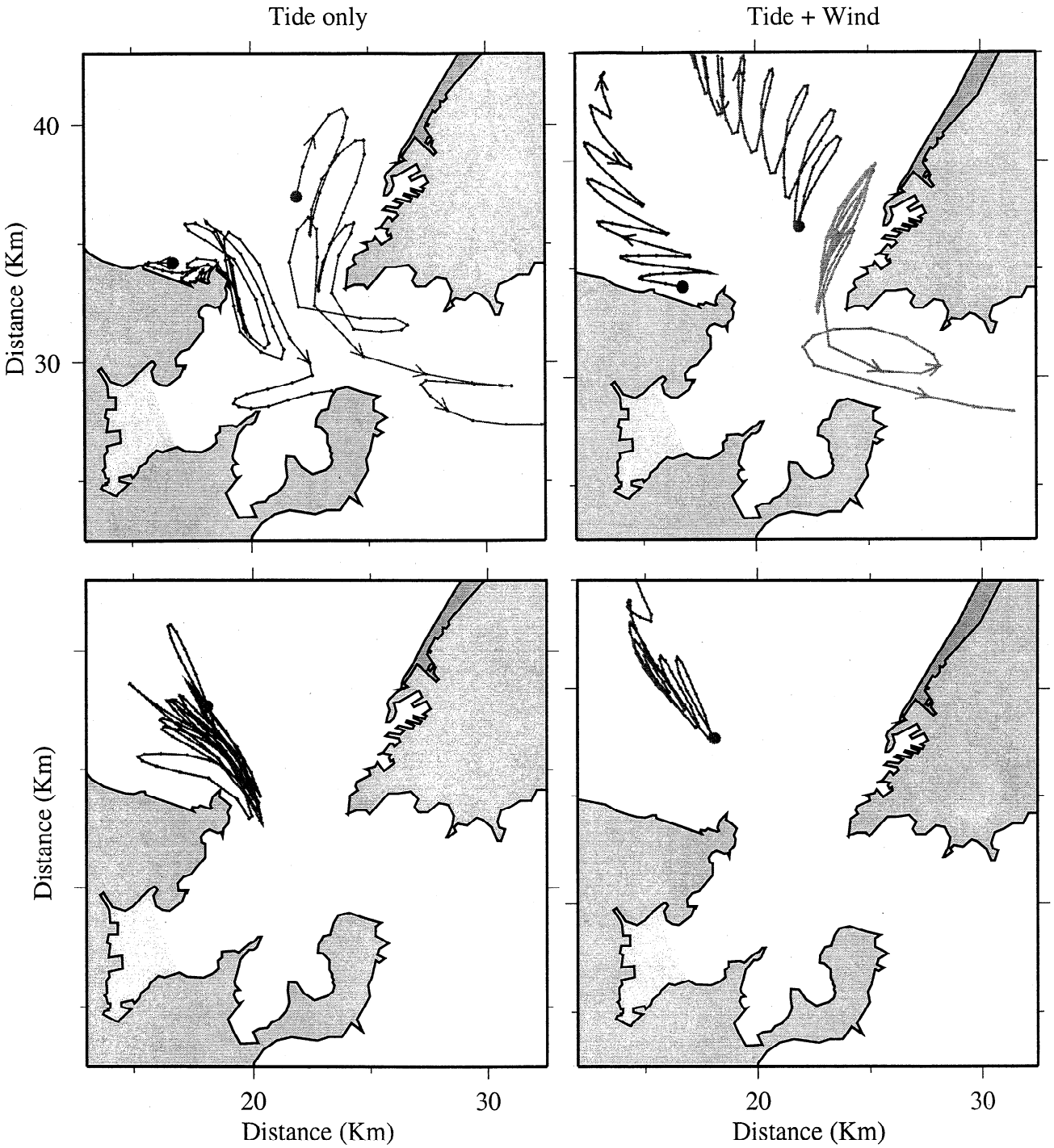

Figure 12. The trajectories of individual particles released at the surface for the case with (left) tide only and (right) tide plus wind. The solid dot is the initial position of a particle. The trajectory of a particle was drawn with a 1-hour time interval. The particle's position at each hour is indicated by a point on the trajectory. The arrow shows the direction of the particle's trajectory.

spatial distribution of phytoplankton remained unchanged, even though its concentration varied remarkably with changes in this parameter. This suggests that our model results for phytoplankton were robust.

6. Summary and Discussion

The marine ecosystem of Jiaozhou Bay was examined using a 3-D coupled physical and biological model. Physical processes included (1) the M_2 tide, (2) river discharges, and (3) wind. The biological model described a simple, phosphate-based, lower trophic *NPZ* food web. The physical model has provided a reasonable simulation of the amplitude and phase of M_2 tide. The model-predicted field of residual current in Jiaozhou Bay was characterized by a clockwise circulation, with a strong eddy in the outer bay between Dashitou and Dagang. The southeasterly wind tended to cause a relatively strong northwestward water transport near the

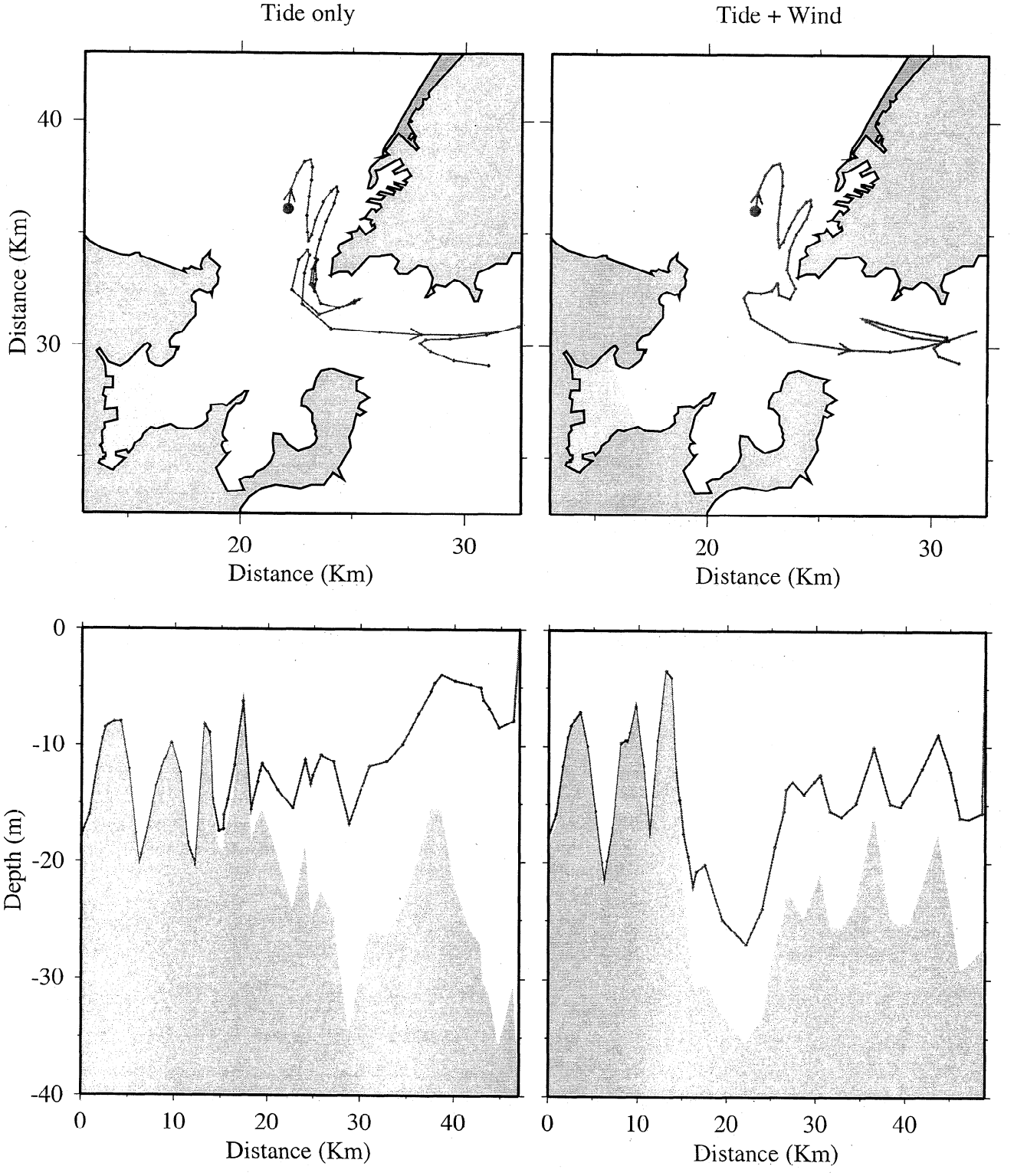

Figure 13. The trajectories of individual particles released near the bottom for the case with (left) tide only and (right) tide plus wind and (top) the plan and (bottom) vertical (along the track) views of the particle's trajectory.

surface, but it did not significantly alter the vertically averaged transport in the bay. Relatively strong salinity fronts formed in the northwestern and northernmost coastal regions near river sources.

The model results revealed that physical processes had a direct impact on temporal and spatial distributions of nutrients and phytoplankton as well as on shellfish aquaculture. Tidal mixing caused both physical and biological variables to be well-mixed in the vertical. The concentrations of nutrients and phytoplankton were high in the northwestern and northern regions of the bay near river sources but decreased from the inner bay to the outer bay. The model results suggested that under a background system with river discharges and tidal mixing, the southeasterly wind, which prevailed over the bay

Table 4. Sensitivity Index of Biological Parameters to the Model Result of Phytoplankton in Sites 1, 2, and 3 in Jiaozhou Bay

Parameter	Sensitivity				
	Site 1	Site 2	Site 3	Site 4	Site 5
		Biological			
λ	0.296	0.264	0.226	0.241	0.236
γ	0.335	0.342	0.338	0.330	0.341
g	0.390	0.370	0.341	0.317	0.361
K_s	0.408	0.365	0.320	0.345	0.328
R_m	0.475	0.460	0.442	0.605	0.465
V_m	1.030	1.101	1.190	1.295	1.130
		Physical			
K_H	0.057	0.023	0.123	0.212	0.043
K_m	0.001	0.003	0.001	0.008	0.012

in summer, may cause an unusual nutrient "accumulation" in the innermost bay, leading to a phytoplankton bloom.

The estimation of nutrient and phytoplankton fluxes in the five given sites suggested that the nutrients in the bay were supplied and maintained directly by physical processes, while the temporal variation of phytoplankton was controlled dominantly by biological processes. In the inner bay, near river sources, the nutrients were directly supplied or maintained by horizontal advection and diffusion, while in the central and outer regions they were mainly controlled by horizontal diffusion. The temporal variation of phytoplankton was directly related to spatial nutrient distributions rather than advection and diffusion. A significant amount of nutrients was advected out of Jiaozhou Bay into the YS. The water exchange between Jiaozhou Bay and the YS was controlled by a chaotic kinematic process associated with the nonlinear interaction between the oscillating tidal currents and double closed residual eddies.

Shellfish aquaculture tended to alter the entire Jiaozhou Bay ecosystem. The loss of phytoplankton in the shellfish aquaculture sites tended to be compensated by phytoplankton flux advected or diffused from the surrounding waters. The large consumption of phytoplankton by shellfish also caused a net flux of phytoplankton into the bay from the YS, even though nutrients were still advected out of the bay.

The fact that a phytoplankton bloom can occur under a condition of southeasterly wind implies that physical processes may have a direct impact on the occurrence of "red tide" along the northern coast of Jiaozhou Bay. The overloading of nutrients from inland shrimp aquaculture, industries, and other urban human activities tended to cause a high nutrient concentration near the inner bay, which provided a favorable condition for eutrophication. The "accumulation" of nutrients near the northern coast due to the southeasterly wind may speed up the eutrophication process and thus caused a sudden occurrence of "red tide."

The model results also suggest that shellfish aquaculture had a direct impact on the bay-scale ecosystem of Jiaozhou Bay. In addition to the eutrophication caused by nutrient loading from inland shrimp aquaculture, industries, and other urban human activities, high densities of suspended feeding bivalves will alter the lower trophic food web environment by a substantial grazing of phytoplankton, excretion, and biodeposition. Aquaculture populations of bivalves tended to transfer large quantities of materials from the water column to the sediment, which may dramatically change the content of organic matter in the benthic layer [*Kautsky and Evans*, 1987; *Kaspar et al.*, 1985). The benthic processes, in turn, may alter nutrient cycling in the bay [*Barg*, 1992; *Dame*, 1993; *Jørgensen*, 1990]. A long-term aquaculture strategy is desperately needed in order to ensure that this area has a well-balanced and healthy marine ecosystem.

It should be pointed out again that our present model has not included the intertidal zone around the coast. Although the influence of the nutrient flux from this zone on Jiaozhou Bay has been indirectly considered in our numerical experiments through river discharges, the direct impact of intertidal processes still remains unclear. A large amount of nutrients can be advected back to the bay during the ebb tide, which may be an another main source of nutrients to Jiaozhou Bay. This question should be addressed in our future modeling studies. (The animation movies of tidal simulation, temperature, phytoplankton, zooplankton, and nutrients, and particle trajectories can be viewed directly at our web site http://whale3.marsci.uga.edu/research_projects/.)

Acknowledgments. The research was conducted as a component of the U.S.-China Cooperative Program on Living Marine Resources (U.S.-China-LMR). The U.S. team was funded by Georgia Sea Grant College Program under grant NA66RG0282. The Chinese team was supported by State Oceanic Administration, P. R. China and National Natural Science Foundation of China under grant 39670580. We also want to thank George Davidson for his editorial help on the manuscript. Two anonymous reviewers have provided many critical comments and constructive suggestions. Their help was greatly appreciated.

References

Barg, U. C., Guidelines for the promotion of environmental management of coastal aquaculture development. *FAO Fish. Tech. Pap., 328*, 1992.

Blumberg, A. F., A primer for ECOM-si, technical report, 73 pp. HydroQual, Inc. Mahwah, New Jersey,. 1993.

Blumberg, A. F., and G. L. Mellor, A description of a three-dimensional coastal ocean circulation model, in *Three-Dimensional Coastal Ocean Model, Coastal Estuarine Sci.*, vol 4, edited by N.S. Heaps, pp.1-16, *AGU*, Washington, D.C.,1987.

Chen, C., and R. Beardsley, Numerical study of stratified tidal rectification over finite-amplitude banks, part I, Symmetric banks, *J. Phys. Oceanogr., 25*, 2090-2110, 1995.

Chen, C., and R. Beardsley, Tidal mixing and cross-frontal particle exchange over a finite asymmetric bank: A model study with application to Georges Bank, *J. Mar. Res., 56(5)*, 1163-1201, 1998.

Chen, C., R. Beardsley, and R. Limeburner, Comparison of winter and summer hydrographic observations in the Yellow and East China Seas and adjacent Kuroshio during 1986, *Cont. Shelf Res., 14*, 909-929, 1994.

Chen, C., R. Beardsley, and R. Limeburner, Numerical study of stratified tidal rectification over finite-amplitude banks, Part II, Georges Bank, *J. Phys. Oceanogr., 25*, 2111-2128, 1995.

Chen, C., D. A. Wiesenburg, and L. Xie, Influences of river discharge on biological production in the inner shelf: A coupled biological and physical model of the Louisiana-Texas shelf, *J. Mar. Res., 55*, 293-320, 1997.

Chen, C., L. Zheng, and J. O. Blanton, Physical processes controlling the formation, evolution, and perturbation of the low-salinity front in the inner shelf off the southeastern U.S.: a modeling study, *J. Geophys. Res., 104*, 1259-1288, 1999.

Collaudin, B, A first approach of aquaculture development in Jiaozhou Bay (P. R. China). *Investigation Report*, IFREMER, France, 1996.

Dame, R. F., The role of bivalve filter-feeder material fluxes in

estuarine ecosystems. in *Bivalve Filter-Feeders in Estuarine and Coastal Ecosystem Processes*, edited by Dame, R. F., NATO ASI Ser., *33*. 245-270, 1993.

Ding, W. A., Tides and tidal currents, in *Ecology and living resources of Jiaozhou Bay*, edited by R. Liu., Science Press, Beijing, pp. 39-72, 1992.

Franks, P. J. S., and C. Chen, Plankton production in tidal fronts: A model of Georges Bank in summer, *J. Mar. Res.*, *54*, 631-651, 1996.

Franks, P. J. S., J. S. Wroblewski, and G. R. Flierl, Behavior of a simple plankton model with food-level acclimation by herbivores, *Mar. Biol.*, *91*, 121-129, 1986.

Gao, S., and K. Wang, Abundance and distribution of zooplankton in Jiaozhou Bay, in *Ecological Study of Jiaozhou Bay*, edited by J. Dong and N. Jiao, pp. 151-159, Science Press, Beijing, 1995.

Guo, Y, and Z. Yang, Plankton, in *Ecology and Living Resources of Jiaozhou Bay*, edited by R. Liu, pp. 136-139, Science Press, Beijing, 1992.

JØrgensen, C. B., Bivalve Filter Feeding: Hydrodynamics, Bioenergetics, Physiology, and Ecology, 140 pp. Olsen and Olsen, Fredensborg, Denmark, 1990.

JØrgensen, S. E., S. N. Niclsen, and L. A. JØrgensen, *Handbook of Environment and Ecological Parameters*, Elsevier, New York, 1991.

Kaspar, H. F., P. A. Gillespie, I. C. Boyer, and A. L. Mckenzie, Effects of mussel aquaculture on the nitrogen cycle and benthic communities in Kenepru Sounds, *New Zealand. Mar. Biol.*, *85*, 127-136, 1985.

Kautsky, N., and S. Evans, Role of biodeposition by Mytilus edulis in the circulation of matter and nutrients in a Baltic coastal ecosystem, *Mar. Ecol. Progr. Ser.*, *38*, 201-212, 1987.

Kawamiya, M., M.. J. Kishi, Y. Yamanaka and N. Suginohara, An ecological-physical coupled model applied to station Papa. *J. of Oceanogr.*, *51*, 635-664, 1995.

Kremer, J. N., and S. W. Nixon, *A Coastal Marine Ecosystem*. 217 pp. Springer-Verlag, New York, , 1978.

Li, C., Grazing of copepods, Master thesis, Inst. of Oceanogr., Chin. Acad. Sin., Qingdao,1997.

Liu, F. and K. Wang, The rivers along Jiaozhou Bay coastal line and their geological effects, *Mar. Sci. (in Chinese)*, *1*, 25-28, 1992.

Liu, R., The natural environmental characteristics of Jiaozhou Bay, in *Ecology and living resources of Jiaozhou Bay*, edited by R. Liu, pp. 2-3, Science Press, Beijing, 1992.

Loder, J. W., Topographic rectification of tidal currents on the sides of Georges Bank, *J. Phys. Oceanogr.*, *10*, 1399-1416, 1980.

Marine Environmental Monitoring Center (MEMC), A comprehensive environmental investigation and study on the Jiaozhou Bay and coastal area, North Sea Branch, SOA. *Mar. Sci. Bull.*, *11*(3), special issue, 76 pp., 1992.

McAllister, C. D., Zooplankton rations, phytoplankton mortality and the estimation of marine production, In: *Marine Food Chains*, edited by J. H. Steele, pp. 472, Univ. of Calif. Press, Berkeley, 1970.

Mellor, G. L., and T. Yamada, Development of a turbulence closure models for geophysical fluid problem. *Rev. Geophys.*, *20*, 851-875, 1982.

Raymont, J. E. G. (Ed.), *Plankton and Productivity in the Oceans*, vol. 2, *Zooplankton*, Pergamon, New York, 1980.

Ridderinkhof, H, and J. T. F. Zimmerman. Chaotic stirring in a tidal system. *Science*, *258*, 1107-1111, 1992.

Shen, Z., The variations of nutrients in Jiaozhou Bay. in *Ecological Study of Jiaozhou Bay*, edited by J. Dong and N. Jiao, pp. 47-52, Science Press, Beijing, 1995.

Steele, J. H., *The Structure of Marine Ecosystems*, 128 pp., Harvard Univ. Press, Cambridge, Mass., 1974.

Steele, J. H., and E. W. Henderson, A simple plankton communities, *Philos. Trans. R. Soc. Lond.*, *280*, 485-534, 1981.

Steele, J. H., and E W. Henderson, The role of predation in plankton models, *J. Plankton Res.*, *14*, 157-172, 1992.

Valiela, I., Nutrient Cycles and Ecosystem Stoichiometry in Marine Ecological Processes, pp. 425-433, Springer-Verlag, New York, 1995.

Wang, R., N. Jiao, C. Li, P. Ji, and Z. Shen, Primary production and new production in Jiaozhou Bay, in *Ecological Study of Jiaozhou Bay*, edited by J. Dong and N. Jiao, pp. 125-136, Science Press, Beijing, 1995.

Weng X., L. Zhu and Y. Wang. Physical oceanography. In: *Ecology and Living Resources of Jiaozhou Bay*, edited by R. Liu, pp. 20-72, Science Press, Beijing, 1992.

Winter, J. E., A review on the knowledge of suspension-deeding in lamellibranchiate bivalves, with special reference to artificial aquaculture systems, *Aquaculture*, *13*, 1-33, 1978.

Wu, Y., and Y. Zhang, Distributional characteristics of chlorophyll-a and primary productivity in Jiaozhou Bay. in *Ecological Study of Jiaozhou Bay*, edited by J. Dong and N. Jiao, pp. 137-150, Science Press, Beijing, 1995.

Yang, H., and Q. Liu, Distribution and variation of particulate organic carbon (POC) and particulate nitrogen (PN) in seawater of Jiaozhou Bay, in *Ecology and Living Resources of Jiaozhou Bay*, edited by R. Liu, pp. 53-61, Science Press, Beijing, 1992.

Zhao, Y., Y. Chen, and Z. Lin, The climate around Jiaozhou Bay. in *Ecological Study of Jiaozhou Bay*, edited by J. Dong and N. Jiao, pp. 8-24, Science Press, Beijing, 1995.

Zimmerman, J. T. F. The tidal whirlpool: A review of horizontal dispersion by tidal and residual currents, *Neth. J. Sea Res.*, *20*(2/3), 133-154, 1986.

C. Chen, R. Ji, L. Zheng, M. Rawson, School of Marine Programs, Marine Science Building, University of Georgia, Athens, GA 30602. (chen@whale.marsci.uga.edu; ji@shark4.marsci.uga.edu; zheng@whale3.marsci.uga.edu; mrawson@arches.uga.edu)

M. Zhu, First Institute of Oceanography, State Oceanic Administration, Qingdao, 266003, People's Republic of China. (qdmyzhu@163.net)

(Received August 6, 1998; revised June 10, 1999;
Accepted May 20, 1999.)